

Response to Reviewers

We would like to thank both reviewers for their time and effort to review our manuscript. We have addressed all major and minor comments raised by the reviewers. In doing so, we feel we have crafted a revised manuscript that is more rigorous in content, and better presents the results of the study. Here we list the main changes that we have made:

- We now include an analysis of the SST, rather than only the RSST, adding 3 new figures, which are the equivalent of the figures 2, 3 and A2.
- We added a time series of the precipitation asymmetry index (PAi) to highlight the ITCZ shift.
- We added three supplementary figures to investigate the ocean temperature anomalies on a transect across the equatorial Pacific.

We did not investigate the impacts of the ocean initial conditions on ENSO, because this study aims to extend previous work that look at the response of single eruptions or a multiple-eruption mean to separate out the role of aerosol distribution of ENSO. The role of the initial conditions is indeed a relevant topic, which we have currently started investigating and will be the focus of a follow-up study.

Below, we copy the reviewers' comments in bold and describe how each of these issues has been addressed in the revised manuscript. The revised version of the manuscript is attached after the answers to reviewers' comments, and the changes compared to the original version are highlighted in bold.

20 **Response to Reviewer #1:**

The reviewed paper deals with a very hot and scientifically important research question of how ENSO responds to hemispherically symmetric and asymmetric radiative forcing caused by the three largest volcanoes of the 20th century, Agung, El Chichon, and Pinatubo. The authors test the hypothesis that the primary driving mechanism is ITCZ's shift that works for symmetric and asymmetric volcanic forcing. The study takes advantage of the unique 200-member ensemble of MPI-ESM 1.1 with a relatively low effective spatial resolution, 180 km x 150 km x 16 layers. The research topic is important, the methods are sound, the results are interesting, but the analysis has significant flaws. Therefore, I suggest the authors conduct a major revision to enhance their analysis and improve the text.

We thank the reviewer for the thorough evaluation of the manuscript and appreciate the positive remarks on the relevance of the study. We went through the analysis of the results (section 3 and 4) to make it clearer and we added the results with the SST and the ocean temperature transects to solidify our analysis.

Major comments:

1. The analysis is based on calculating the ensemble average responses to volcanic forcing. It is known that ENSO response to volcanic forcing is sensitive to the ocean preconditioning. The used approach averages out responses to individual initial conditions (El Nino, La Nino, or neutral), potentially removing the effect of the mechanisms that depend on preconditioning, e.g., ocean dynamical thermostat (ODT).

We agree with the reviewer that the initial conditions of the ocean before the eruptions have an impact on the ENSO response and that is a relevant aspect of the ENSO response to volcanic eruptions. However, our main object is to investigate the impact of different aerosols distributions (NH, SH and evenly distribution) rather than the impact of the initial conditions that is a matter of a follow-up study. Moreover, it is common to average the response of different initial conditions and investigating the averaged result when the objective is to present the response of ENSO to asymmetric forcing (e.g. Pausata et al., 2015; Stevenson et al., 2016; Zuo et al., 2018).

2. Nino3.4 index based on relative SST exaggerates the El Nino-like response. A comparative analysis with the regular SST is needed.

Following the reviewer suggestion, we added the analysis only looking at the SST (Fig A11, A12, A13). The results are really similar to the RSST except that the El Niño-like anomalies are, as expected, less strong since they are partly masked by the volcanically induced cooling. We have added the following comment in the manuscript comparing the RSST to the SST in the results section.

50

“The results using the SST (Figs. A11, A12 and A13) are qualitatively similar to the RSST (Figs. 2, 3, and A3), but the El Niño-like anomalies are less strong since they are partially masked by the global cooling induced by the stratospheric aerosols which is in agreement with other studies (Khodri et al., 2017; Maher et al., 2015).”

55

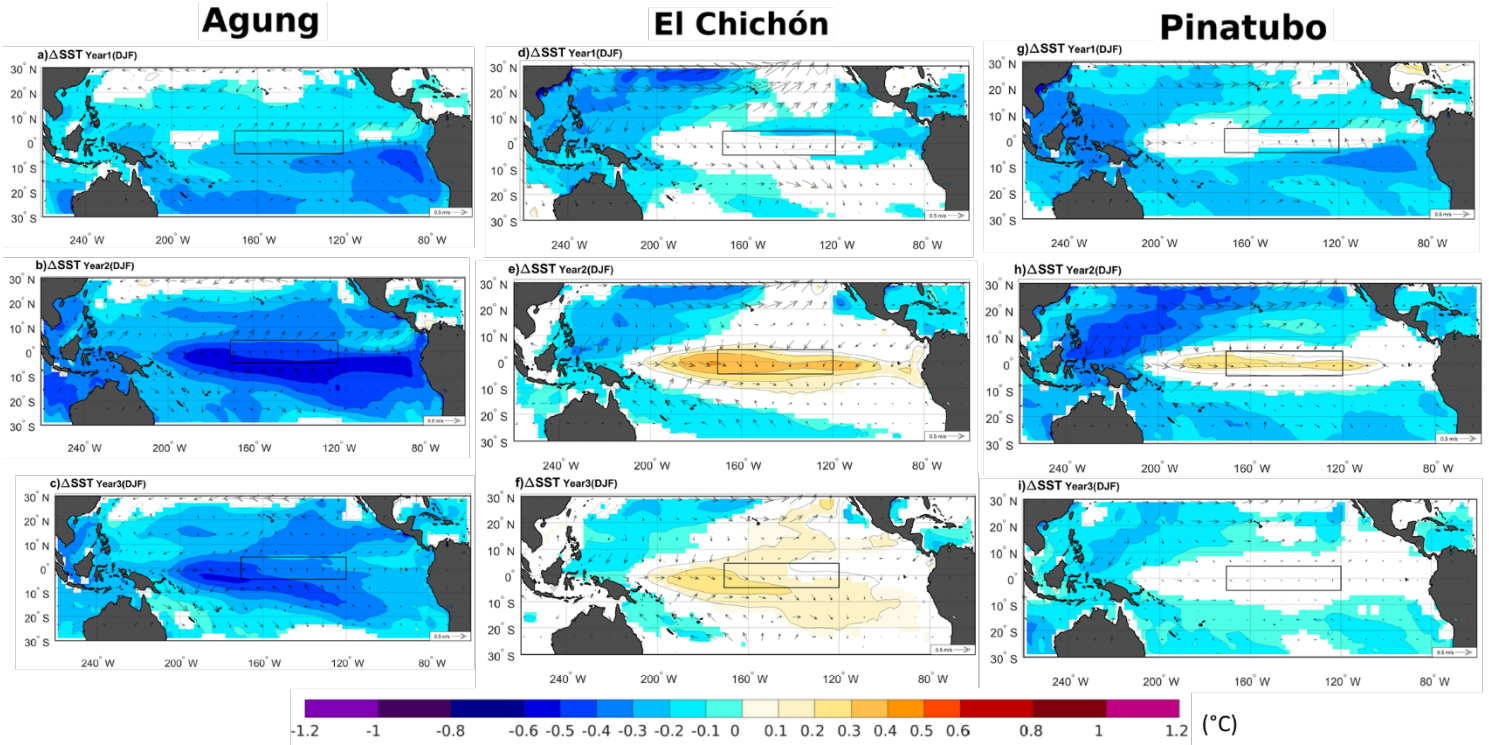


Figure R1 : Ensemble mean of changes in sea surface temperature (SST) (shadings) and 10 m winds (arrows) between the volcano case and the climatology for each of the following three winter season (DJF) after the Agung (a-c), El Chichón (d-f) and the Pinatubo (g-i) eruptions. Only significant SST changes are shaded with an approximate 95 % confidence level using a Student t-test. Contours show the SST anomalies following the color bar scale (solid lines for positive anomalies and dashed lines for negative anomalies, the 0 line is omitted). The boxes indicate the Niño 3.4 area

60

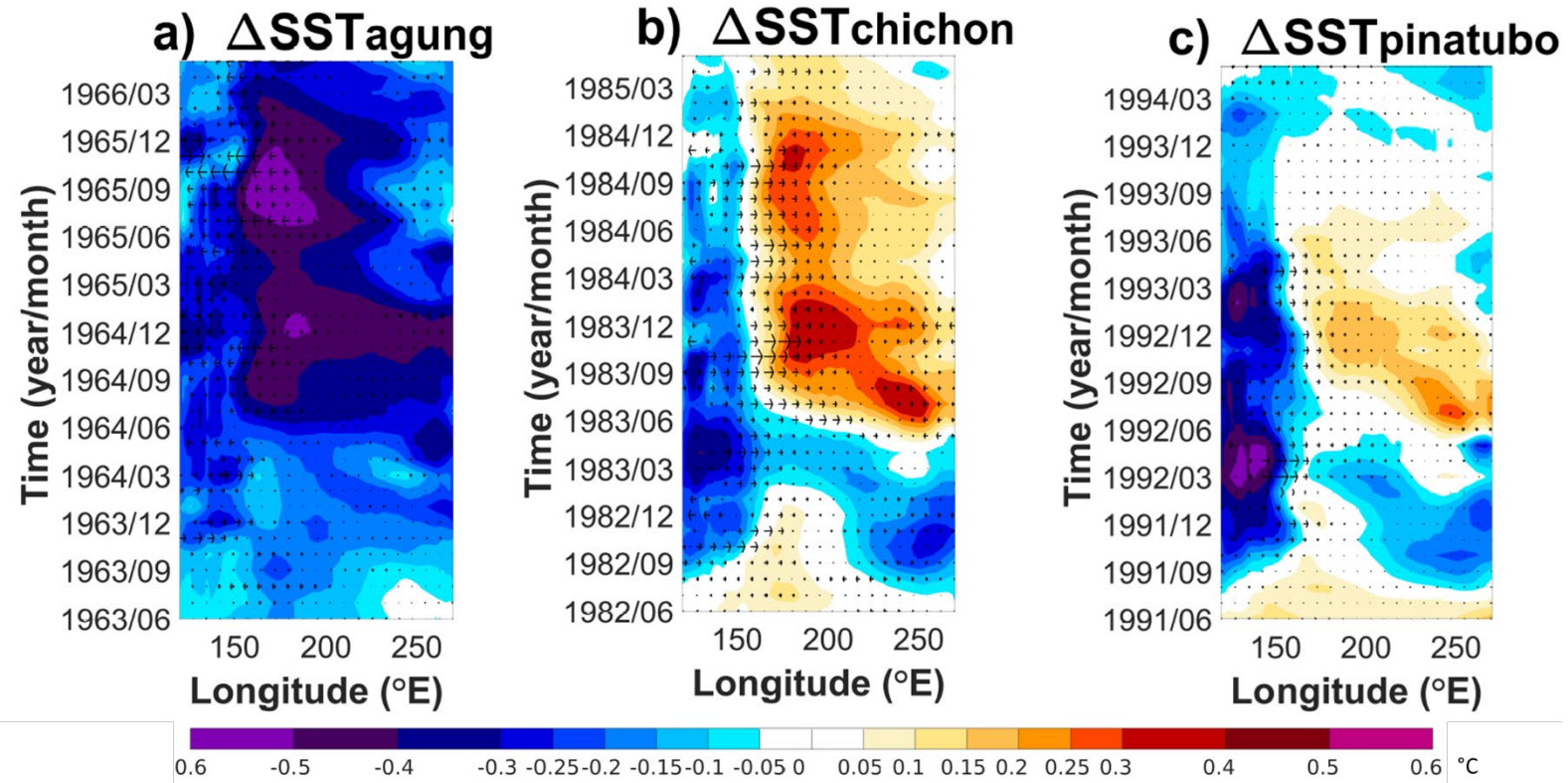
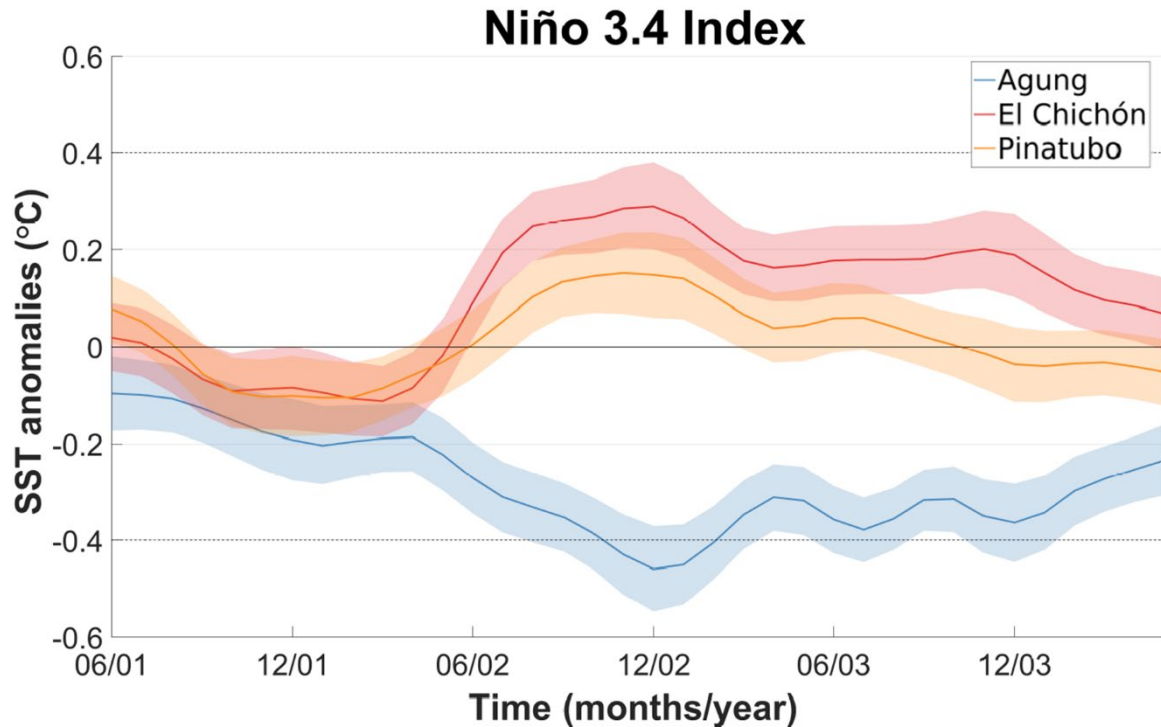


Figure R2: Hovmöller plot of the ensemble mean of the SST anomalies in the equatorial Pacific (averaged over -5°N and 5°N) and the change in the zonal component of the 10 m winds (m/s) for the three years following each eruption. The anomalies are calculated relative to the three years before each eruption.



75

Figure R3: Ensemble mean changes in the Niño 3.4 index after each eruption. The 3-year climatology is subtracted to calculate the anomalies. Shading represents twice the standard error of the mean using an approximate 95% confidence interval.

80 **3. Both EL Chihon and Agung eruption happened before the spring predictability barrier when ENSO responses are unstable. So, the responses to these two eruptions are contaminated by stochastic ENSO behavior.**

While El Chichon and Agung eruptions did occur before the spring predictability barrier, the effect of the eruption and its associated aerosol loading is not limited to the time of the eruption. As it is possible to see from the AOD figure (Fig.1), the aerosol loading peaks in summer and high aerosol concentrations persist for a couple of years. In addition to that, given the

85 large ensemble used in this study, the stochastic ENSO behaviour is filtered out (see also Milinski et al., 2019).

4. ENSO's response to the Agung 1963 eruption, which is a milestone in the authors' arguments, is not what they think. It is not La Nina like a response, as its spatial temperature pattern dislikes the La Nina one. The ocean cooling in the Southern Hemisphere caused by Volcanic forcing that expands to the Northern Hemisphere could explain it. It is why

90 **it takes three years.**

The reviewer is not convinced that the spatial temperature pattern is La Niña-like, arguing that the cooling over the equatorial Pacific could just simply due to the direct cooling induced by the eruption. We thank the reviewer for raising this point as the

analysis of the ocean transect along the equator across the tropical Pacific further strengthens our main conclusion (Figures A14, A15 and A16). We note that this analysis only includes 100-ensembles members due to data availability.

95 The temperature anomalies following Agung (Fig. A14) are not just superficial but extend down to 200 m depth. The warming below 100 m in the western Pacific is typical of an ongoing La Niña, as well as the cooling on the eastern side along the thermocline (increased upwelling). Furthermore, one can appreciate that the El Chichón and Pinatubo show indeed the opposite anomalies compared to Agung (Figs. A15 and A16). For example in the El Chichón case one can clearly appreciate the superficial cooling induced by the volcanic eruption on year 1, as a warming pattern is simulated along the thermocline on the eastern Pacific (typical of El Niño), but no warming at the surface is present.

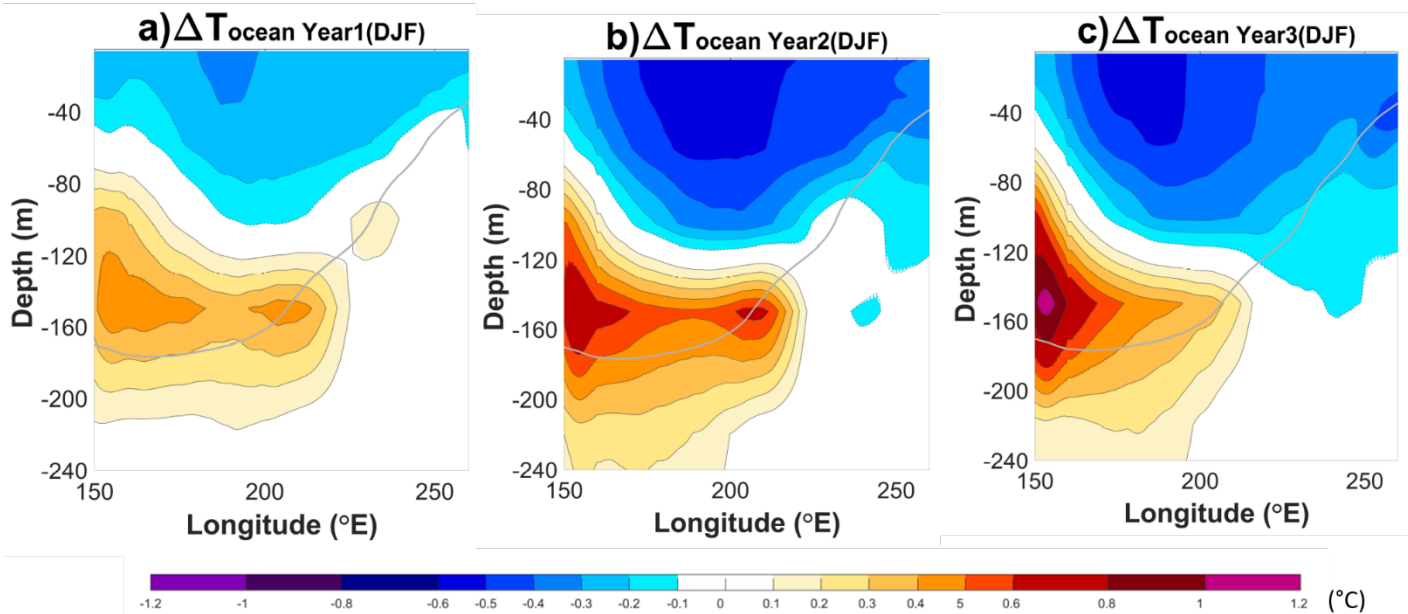
100 The wind anomalies following Agung (see Fig. 2) are also opposite compared to El Chichón, hence leading to opposite upwelling conditions along the equator, further corroborating that the temperature anomalies are mostly dynamically driven. Therefore, this analysis strengthens our main conclusion on the role of the ITCZ in explaining the ENSO response to different aerosol distribution.

105 Furthermore, if the ENSO response were not dynamically driven (i.e. due to the induced changes in upwelling caused by wind anomalies), one would wonder why for Agung the aerosol loading over the equator does lead to a cooling extending deeper into the ocean, but a similar aerosol loading for El Chichón does not.

110 Finally, we are not sure how the ocean cooling in SH could expand to the NH (if it were not for dynamical reasons as the aerosol is confined to the SH). From figure R7, it is possible to see that the cooling “expanding” to the NH is just the La Niña associated with the negative PDO pattern. To further strengthen the fact that those anomalies are indeed La Niña, we have performed a composite of all La Niña events occurring in the 4 years before each eruption (i.e. 12 years) for 100 ensemble members (total of 1200 years and 237 La Niña events). As shown in figure A17 the pattern is remarkably similar to what shown following the Agung eruption. Therefore, we can confidently assert that the Agung eruption triggered a La Niña response in our model simulation.

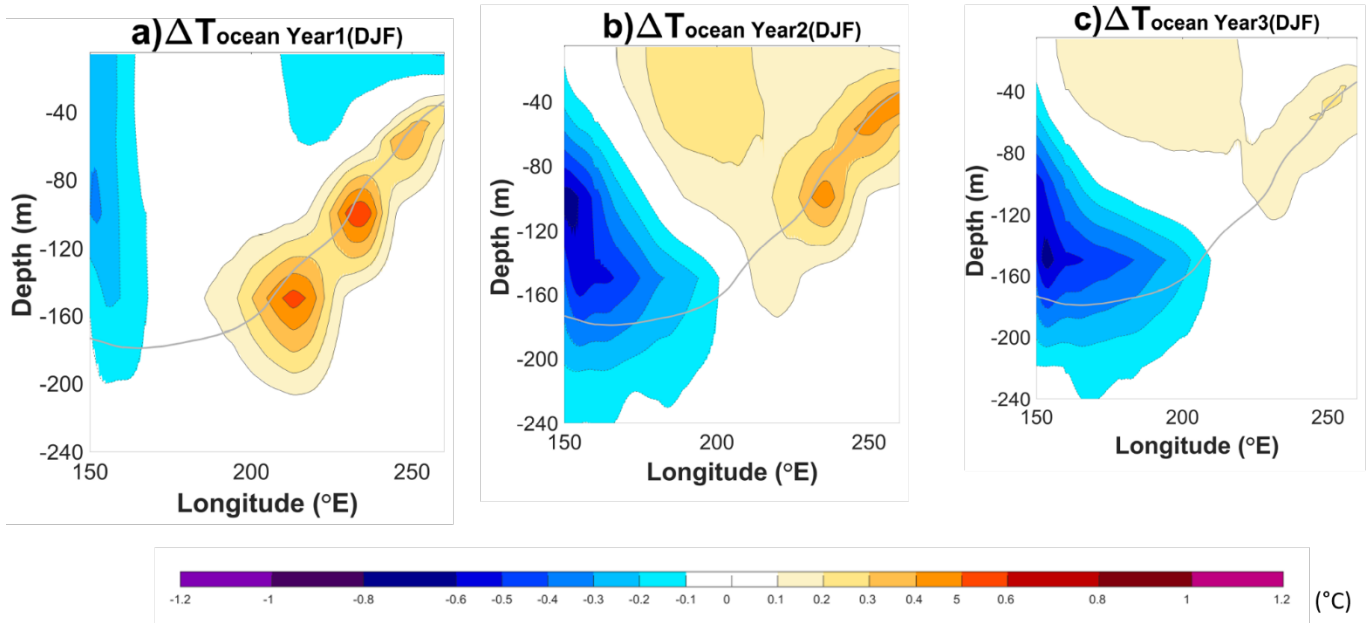
115

Agung

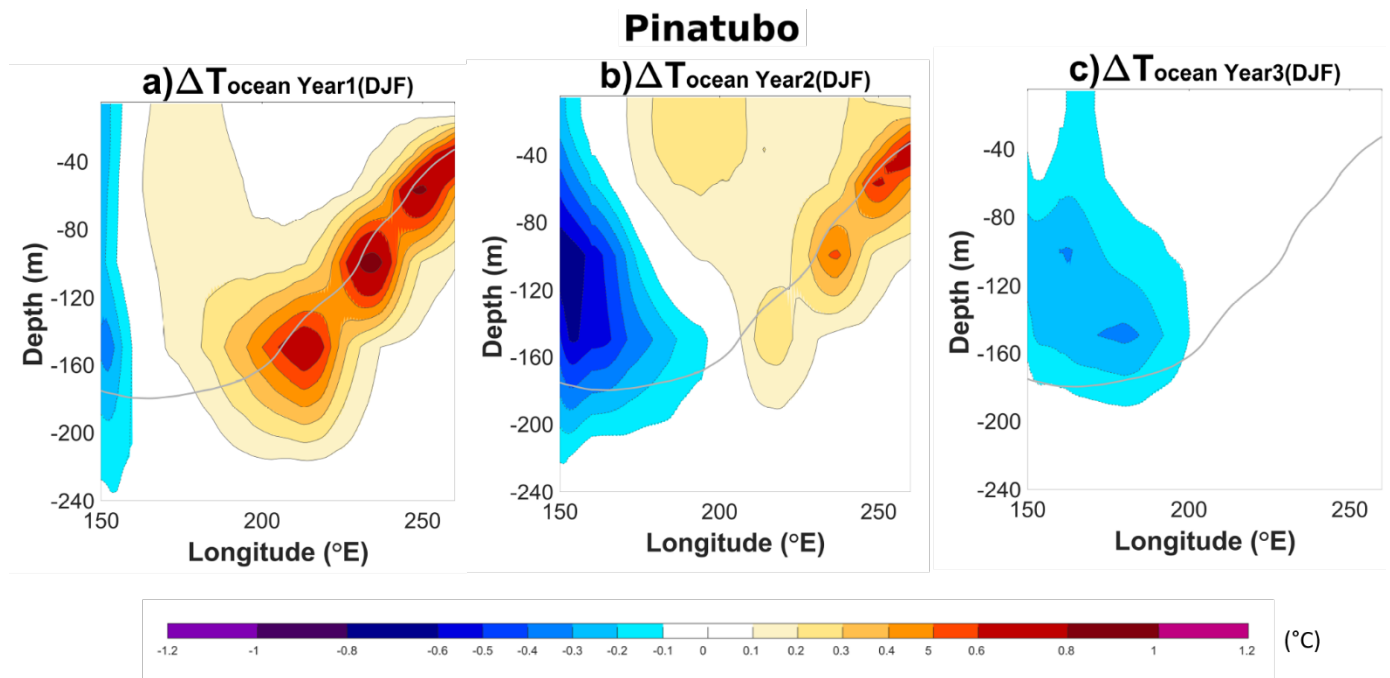


120 **Figure R4:** Ensemble mean changes shown for a transect in the equatorial Pacific (averaged $5^{\circ}\text{N} - 5^{\circ}\text{S}$) of the ocean temperature (shadings) between the volcano case and the climatology for each of the following three winter season (DJF) after the Agung eruption. Contours show the SST anomalies following the color bar scale (solid lines for positive anomalies and dashed lines for negative anomalies, the 0 line is omitted). The bold grey line shows the climatological thermocline depth (as defined using the 20°C isotherm). This is shown for 100 ensemble members.

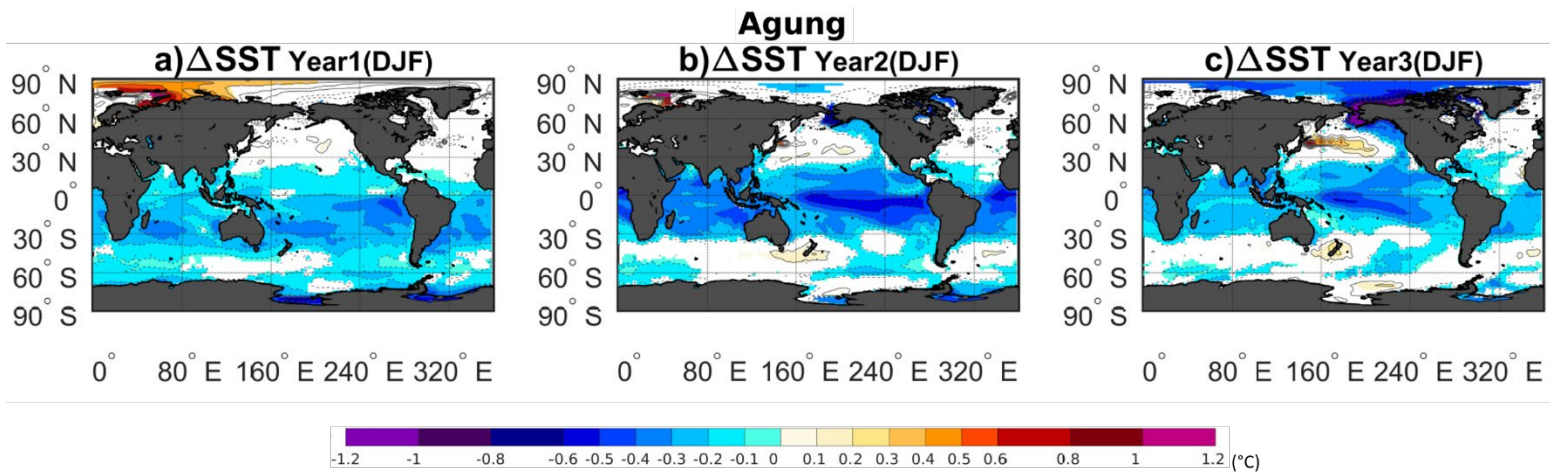
El Chichón



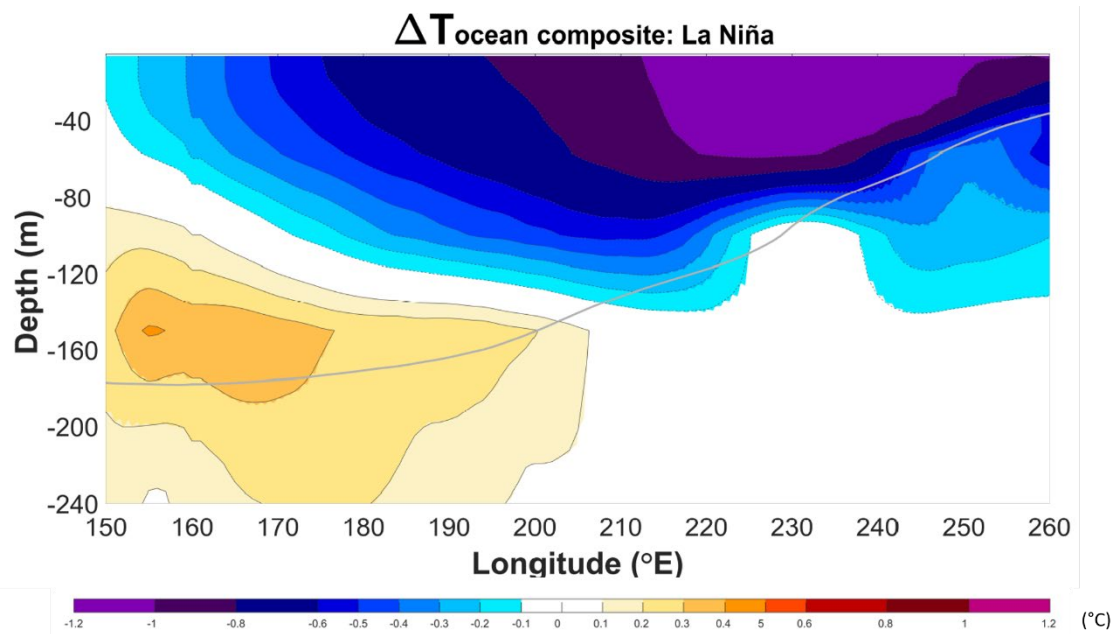
125 **Figure R5:** Ensemble mean changes shown for a transect in the equatorial Pacific (averaged $5^{\circ}\text{N} - 5^{\circ}\text{S}$) of the ocean temperature (shadings) between the volcano case and the climatology for each of the following three winter season (DJF) after the Chichón eruption. Contours show the SST anomalies following the color bar scale (solid lines for positive anomalies and dashed lines for negative anomalies, the 0 line is omitted). The bold grey line shows the climatological thermocline depth (as defined using the 20°C isotherm). This is shown for 100 ensemble members.



130 **Figure R6:** Ensemble mean changes shown for a transect in the equatorial Pacific (averaged $5^{\circ}\text{N} - 5^{\circ}\text{S}$) of the ocean temperature (shadings) between the volcano case and the climatology for each of the following three winter season (DJF) after the Pinatubo eruption. Contours show the SST anomalies following the color bar scale (solid lines for positive anomalies and dashed lines for negative anomalies, the 0 line is omitted). The bold grey line shows the climatological thermocline depth (as defined using the 20°C isotherm). This is shown for 100 ensemble members.



135 **Figure R7:** Ensemble mean of the changes in surface temperature between the climatology and the volcano case for each seasons of the year after Agung eruption. Only significant anomalies are shown with an approximate 95% confidence level using a Student t -test. Contours show temperature and precipitations anomalies following the color bar scale (solid line for positive anomalies and dashed line for negative anomalies).



140 **Figure R8:** Temperature composite of La Niña events (Nino3.4 index $< -0.4^{\circ}\text{C}$) for a transect in the equatorial Pacific (averaged between 5°S and 5°N) in the reference period of each eruptions (4 years before each eruptions) and for the winter season (DJF). 100 ensemble members are considered, leading to a total of 1200 year as reference period and 237 La Niña events. Contours show the SST anomalies following the colorbar scale (solid lines for positive anomalies and dashed lines for negative anomalies, the 0 line is omitted). The bold grey line shows the climatological thermocline depth (as defined using the 20°C isotherm).

145 **Minor Comments:**

Fig. 1: Is it AOD from the model? Is it prescribed? From what data set? The color bar is wrong. AOD is an order of magnitude larger.

We thank the reviewer for this useful comment, we were using a wrong spectral band for the AOD we fixed this problem in figure 1 and figure A6. In the methodology section we now read:

150

“The stratospheric aerosols used in this study are prescribed in the historical simulations of the model (MPI ESM) from the data set of Stenchikov et al. (1998) (Giorgetta et al., 2013).”

L36 and L89: The eruption started in February. The major emissions happened in March. Please use the month of the eruption consistently.

155

Thank you for pointing that out, it has been changed in the revised manuscript.

L39-44: RSST enhances the positive signal. Please show the regular SST results for comparison.

We now included the SST (Figs. A11, A12 and A13) and we changed the terms La Niña-like and El Niño-like to relative La Niña-like and relative El Niño-like throughout the manuscripts.

160

L70: Khodry et al. (2017) do not say anything about Walker Circulation. They claim that the atmospheric Kelvin wave does the job.

Thank you for pointing that out, Khodri et al. indeed refer to the fact that tropospheric *heating* anomalies in tropical Africa generate anomalous atmospheric Rossby and Kelvin waves. Although they did not explicitly mention it, these anomalies consequently affect the Walker Circulation as they alter the trade winds and lead to an El Niño-like response (see Fig 7 in Khodri et al. (2017)). The Walker Circulation can be seen as a stationary Kelvin wave (see for ex. Stechmann & Ogrosky (2014)). It now reads:

165

“Khodri et al. (2017) have invoked atmospheric teleconnections associated with the volcanically induced cooling of tropical Africa and weakening of the West African monsoon, which favours anomalous Rossby and Kelvin waves. These anomalous waves alter the Walker circulation and were identified as the primary cause of the post-eruption El Niño-like anomalies.”

170

L121: Response on the 3rd year is too late even for ENSO responses driven by ocean Kelvin Wave propagation.

We agree with the reviewer that the response on the 3rd year is too late for the ENSO response driven by ocean Kelvin Wave propagation. However, we are arguing that the ENSO response is driven by the ITCZ shift and not the Kelvin wave propagation due to the cooling of North Africa. Therefore, in Fig. 5 we see that there is still a strong northward shift of the ITCZ during

175

the 3rd years after the Agung and westward wind anomalies associated to this shift. For the Agung the global cooling last well into the third year and so does the asymmetric cooling of the hemispheres (Figs. A1 and 4).

180

L145-149: The response to the 1963 Agung eruption, as it is shown in Fig 2abc, is not a negative ENSO pattern. It is an ocean cooling but of different origin. It brakes the entire reasoning about the general applicability of the "ITCZ" mechanism.

As mentioned in the major issues we added in the appendix an ocean transect of the ensemble change in the ocean temperature (Fig. A14) that confirm that the ocean cooling after Agung is indeed due to a change in the ENSO state and not only a superficial cooling due to the presence of volcanic aerosols in the stratosphere. We also added a paragraph in the results:

185

190

195

“Furthermore, the temperature anomalies following the Agung eruption are not just superficial but extend down to 200 m depth (Fig. A14). The warming below 100 m in the western Pacific and the cooling along the thermocline in eastern side of the basin are typical of an ongoing La Niña: the pattern is indeed remarkably similar to a composite of La Niña events occurring in the reference periods before the three eruptions (Fig. A17) . On the other hand, the temperature anomalies for the El Chichón and Pinatubo eruptions show opposite results as expected under El Niño conditions (Figs. A15 and A16). Moreover, the wind anomalies following Agung (see Fig. 2 and 3) are opposite compared to El Chichón, hence leading to opposite upwelling conditions along the equator, further corroborating that the ocean temperature anomalies are mostly dynamically driven through the Bjerknes feedback (Bjerknes, 1969).”

L167: Why the reduction in precipitation should favor Rossby waves generation? Decreasing the release of latent heat should decrease the Rossby wave generation.

200

205

From Khodri et al.(2017) “..., it is hence the cooling over the largest tropical landmass, namely Africa, that has the strongest effect on Pacific winds (Fig. 5c). Indeed, the land surface cooling is maximum in the tropics during the first boreal summer and fall (Fig. 4j) and leads to a reduction of the West African monsoon (Fig. 6a, b). The reduced precipitation and tropospheric heating in the equatorial latitudes drive a Matsuno–Gill response^{39, 40} where atmospheric equatorial Rossby and Kelvin waves induce easterly wind anomalies over the Atlantic and westerly wind anomalies over the Indian Ocean and western Pacific (Figs. 6a, b and 7 and Supplementary Fig. 11). This Kelvin wave suppresses convection along its path, with reduced convection over the western Pacific that further strengthens the westerly wind signal (Fig. 6a, b).”

We have modified the sentence to read:

210

“More specifically, the reduction of the tropical precipitation and tropospheric cooling favours anomalous atmospheric Rossby and Kelvin waves in autumn (SON), with a weakening of the trade winds over the western Pacific, leading to El Niño-like conditions in the year after the eruption.”

L185-186: For completeness of the analysis, it would be useful to have these experiments for this paper.

215 While we agree with the review that such ad hoc sensitivity experiments will be useful, we do not have at the moment the computational resources to run them, keeping in mind that we are talking about 200 ensemble simulations.

L210: In this particular model.

Thank you for pointing that out, it has been changed in the revised manuscript.

220 **L225: Adams et al. saw the signal in two years after an eruption (year 0 and year 1).**

Thank you for pointing that out. We have modified the sentences to read:

225 *“Furthermore, our model suggests the peak in ENSO anomalies to be on the second or third year after the eruption as in most modeling studies (Khodri et al., 2017; Lim et al., 2016; McGregor & Timmermann, 2011; Ohba et al., 2013; Stevenson et al., 2017), which is at odds with the reconstructions and observations that see a peak in ENSO anomalies in the first winter following the eruption (McGregor et al., 2010; 2020) and possibly extending to the second year (Adams et al., 2003). The delayed ENSO response in our model simulations relative to reconstructions and observations may be related to the apparent lack of extratropical-to-tropical teleconnections (Pausata et al., 2020) that could favour El Niño-like response already on the first winter following the eruption or other biases within the climate models (e.g., double ITCZ).”*

230

Response to Reviewer #2:

This study investigates the controversial topic of the influence of volcanic aerosol radiative forcing on ENSO. Model studies have suggested that volcanic forcing has a significant impact on tropical ocean-atmosphere circulation which manifest as anomalous ENSO signals. This study uses a very large ensemble of historical simulations, and explores the ENSO response to 3 large tropical eruptions, Agung, El Chichon, and Pinatubo, which each had contrasting spatial distributions of the aerosol forcing. The study shows a strong difference in ENSO response for the Agung eruption vs the other two eruptions, and links this difference in response to the differences in forcing structure. The authors then argue that this result supports a hypothesized mechanism linking volcanic aerosol forcing and ENSO, namely that hemispherically asymmetric forcing leads to a latitudinal shift in the ITCZ, leading to anomalous zonal winds at the equator, and related changes in ocean current and SSTs.

The topic is certainly an active area of research that fits well in the scope of ESD. The model ensemble utilized is impressive in its size, which adds much to the statistical significance of results and aids the study to be able to contribute to the debate. However, the analysis does not sufficiently support the conclusions made, and I suggest the authors undertake major revisions before publication.

We thank the reviewer for the thorough evaluation of the manuscript and appreciate the positive remarks on the pertinence of the study. We went through the analysis of the results (section 3 and 4) to make it clearer and we added a time series of the precipitation asymmetry index (PAi) to support our conclusions.

250 Major comments:

1. The main conclusion of the work is that the ENSO response is driven by the volcanically induced displacement of the ITCZ. It is not, I think, so clearly stated, but the implicit argument seems to be that the “other” proposed mechanisms such as ODT should depend only on the magnitude of the tropical forcing. The fact that different spatial patterns of forcing lead to (what appear to be) nearly opposite ENSO responses in the model results shown does seem to be a valid challenge to the ODT mechanism hypothesis. But, that in no way proves that the ITCZ mechanism is correct. This would only be the case if there were absolutely no chance of any other mechanism being important, and that is difficult to prove. There is not any strong evidence shown that the ITCZ shift actually happens, let alone that it is the cause of ENSO (or relative ENSO) anomalies. As a result, this main conclusion is not well supported by the results shown.

We agree with the reviewer that there may be additional mechanisms at play; however, the ones that are currently most used (ODT, cooling of the Maritime Continent or of tropical Africa) are not supported by our model results for the reasons explained in the text (see L184 to L189 for ODT; see L190 to L197 for the Maritime Continent and see L198 to L207 for the tropical Africa cooling respectively). Among the possible mechanisms, only the ITCZ shift is fully supported by our results, in particular, the opposite results of El Chichón and Pinatubo vs. Agung. Moreover, our conclusions are that the ITCZ shift is the

dominant mechanism (not the exclusive one) that drives the post-eruption ENSO response because of the significant opposite response to the different volcanic forcing (NH, symmetrical and SH) over the 200 ensemble members. Nevertheless, we have
265 toned down our conclusions and opened up for possible additional mechanisms, as we believe that more studies should indeed be done to investigate the ENSO response to volcanic eruptions.

Regarding the lack of evidence of ITCZ shift, we believed we have provided significant evidence for this. In particular: in figure 6 where it is possible to see the zonal rainfall anomalies and the opposite response for El Chichón and Pinatubo (with a
270 significant increase of the precipitation south of the ITCZ and a significant decrease north) vs. Agung (with a significant increase of the precipitation north of the ITCZ and a significant decrease south); in figure 5 where the spatial distribution of the rainfall anomaly is shown, with a dipole pattern. It has been widely shown in the literature that ITCZ shifts occur as a direct thermodynamical response to differential/asymmetric cooling of the hemispheres (Kang et al., 2008; Schneider et al., 2014); this consequently do affect the trade winds and in turn, via the well-established Bjerknes feedback, the ENSO (Bjerknes, 1969).
275 Nevertheless, to further highlight the ITCZ shift and weakening we have performed additional analysis using the asymmetric precipitation index (Fig. 7).

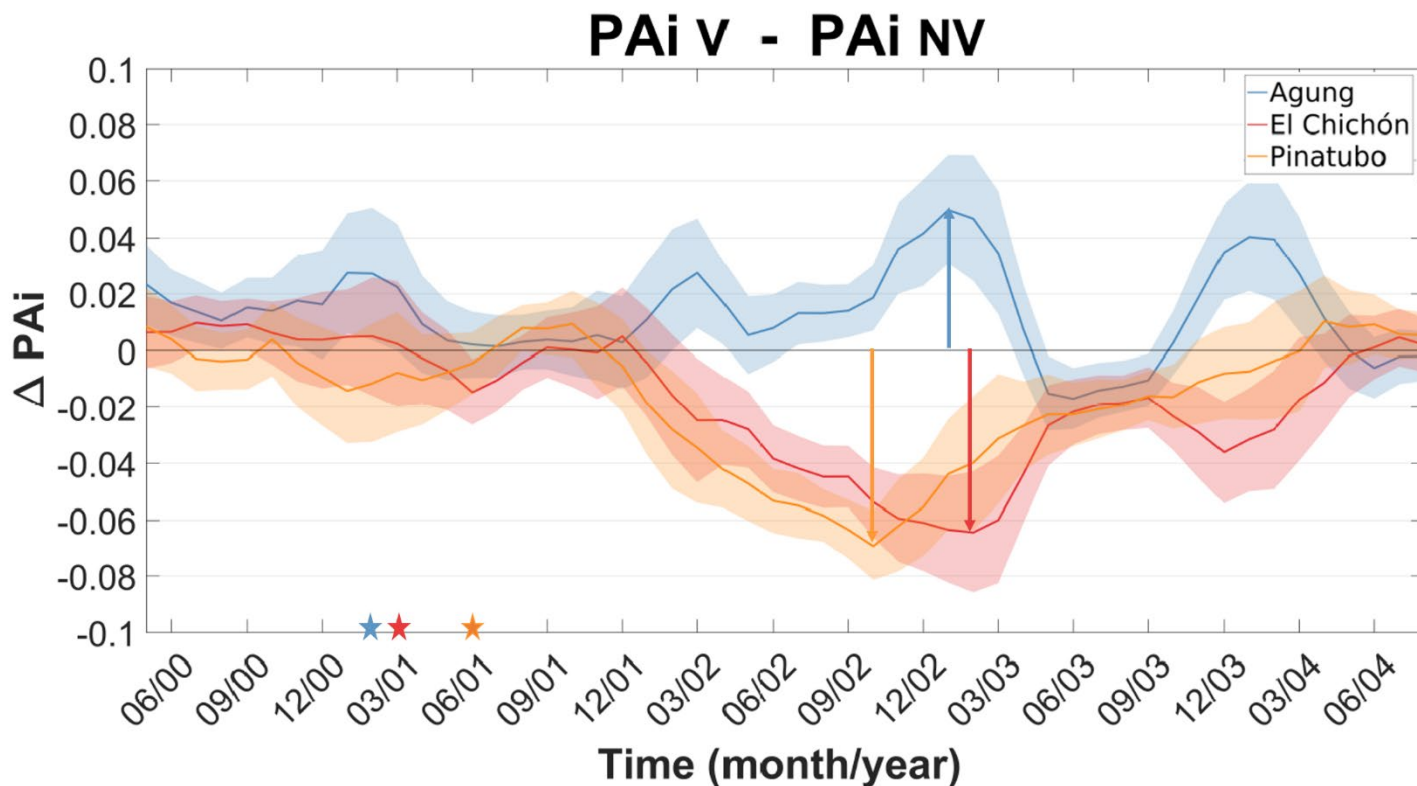


Figure R7: Evolution of the difference in the ensemble mean between the precipitation asymmetry index (PAi) after each eruption (PAi_t), and the climatology (PAi_{NV}). Shading represents twice the standard error of the ensemble mean (i.e. 95% confidence interval). The three stars represents the moment of each eruption.

In figure 7, we have calculated the precipitation asymmetry index in the same way of Colose et al. (2016) but around the average climatological mean of the ITCZ in our model, which is roughly 10 °N. So the expression is given by :

$$PAi = \frac{P_{20^{\circ}N-10^{\circ}N} - P_{10^{\circ}N-Eq}}{P_{20^{\circ}N-Eq}}$$

A positive PAi represents stronger precipitation north of the ITCZ and a negative PAi represents stronger precipitation south of the ITCZ. In figure 7, if the variation of the PAi is positive, it means that there is an augmentation of the precipitation north of the equator which indicates a northward shift of the ITCZ position. In the same way, if there is a negative variation of the PAi, there is a southward shift of the ITCZ. Our results confirm the opposite response in the ITCZ shift between Agung and El Chichón/Pinatubo. For Agung there is a significant northward shift of the ITCZ and for El Chichón and Pinatubo there is a significant southward shift of the ITCZ that peaks in the winter of the second year after the eruption (DJF year2). The inclusion of this figure in the main results support our initial claim that there is a ITCZ shift associated with these eruptions. In the results section we now read:

“Moreover, the precipitation asymmetry index (PAi) (Colose et al., 2016) further highlight the ITCZ shift and weakening (Fig. 7). The expression for the PAi is given by:

$$PAi = \frac{P_{20^{\circ}N-10^{\circ}N} - P_{10^{\circ}N-Eq}}{P_{20^{\circ}N-Eq}}$$

It represents the variation of the zonal precipitation around the average climatological mean of the ITCZ in our model, which is roughly 10 °N. In figure 7, the positive variation of the PAi after Agung eruption means a northward shift of the ITCZ and the negative variations of the PAi after Pinatubo and El Chichón eruptions means a southward shift of the ITCZ. “

Minor comments:

L10 (and title): the paper focuses mostly on the *relative* ENSO, based on RSST anomalies. It is, I think, critically important to be clear with statements whether you refer to ENSO or relative ENSO. While the simulations show positive relative ENSO responses, the absolute SST anomalies seem to be small in this case, so, if ENSO is defined only by the Nino3.4 temperature index, these wouldn't qualify as positive ENSO. To put it another way, even a reader who is familiar with the topic would assume from this abstract that the model produces positive Nino 3.4 temperature anomalies from NH or symmetric forcings, which I believe is incorrect.

We agree with the reviewer and we replaced ENSO response to relative ENSO response in the manuscript. We also included
310 the analysis with the SST and the ocean temperature transects in the appendix to show that the RSST results are similar than
the SST results but just partially masked by the volcanic cooling and that the anomalies are dynamically driven by an alteration
of the ENSO state.

**L12-13: “El Nino-like” or “La Nina-like” is used many times through the manuscript, without any description of what
315 it means in comparison to the “actual” El Nino or La Nina. Why is it only “like” these things? How is it similar and/or
different?**

We thank the reviewer for pointing that out as “El/La Niño/a-like” has been widely used in the literature with different
meanings (in particular model vs. proxy community). We have added a new sentence in the introduction (section 1) of the
revised manuscript to clarify this point:

320

*“The terms El Niño-like and La Niña-like conditions are used in the context of modeling studies to describe an anomalous
warming or cooling of the equatorial Pacific relative to the reference case.”*

L13: again, I think you mean relative anomaly here?

325 We thank the reviewer for pointing that out, we are now referring to relative anomalies throughout the manuscript.

**L26: The atmospheric and ocean responses to volcanic forcing are difficult to prove from observations due to the
limited sample size, and evidence for their existence is largely from models, which are imperfect. It’s important not to
overstate our confidence in the existence of these responses.**

We have rephrased the sentence to read:

330 *“These rapid modifications in temperature may induce dynamical changes in the atmosphere and in the ocean such as a
strengthening of the polar vortex ...”*

L19: I don’t this Robock 2000 says this explicitly.

We have changed the sentence to read:

335 *“Aerosol particles from volcanic eruptions are one of the most important non-anthropogenic radiative forcing that have
influenced the climate system in the past centuries (e.g., Robock, 2000).”*

**L31: Discussion of paleoclimate proxies should include the paper from Dee et al.
(2020):**

340 **Dee, S. G., Cobb, K. M., Emile-Geay, J., Ault, T. R., Lawrence Edwards, R., Cheng, H. and Charles, C. D.: No consistent ENSO response to volcanic forcing over the last millennium, Science (80-.), 367(6485), 1477–1481, doi:10.1126/science.aax2000, 2020.**

We thank the reviewer to bring this new paper that add more debate on this controversial subject. We now read in the introduction :

345

“Paleoclimate archives and observations from the past centuries suggested that large tropical eruptions are usually followed by a warm sea-surface temperature (SST) anomaly in the Pacific (e.g., Adams et al. , 2003; D’Arrigo et al. , 2005; Li et al., 2013; S. McGregor et al. , 2010; Wilson et al., 2010) even if there is still uncertainty on the significance of theses results (Dee et al., 2020).”

350

L39: Reference should be made in the paragraph to the analysis of CMIP5 models by Paik et al (2019): Paik, Seungmok, et al. "Volcanic-induced global monsoon drying modulated by diverse El Niño responses." Science Advances 6.21 (2020): eaba1212.

We thank the reviewer for bringing this recent paper to the discussion.

355

L35: Please replace instances of “Krakatoa” with the preferred “Krakatau”

We changed the occurrence of “Krakatoa” to “Krakatau”

L40: “Most recent” does not necessarily mean most correct. Also, you say “studies” but cite only one paper.

360 We agree with the reviewer that most recent studies does not necessarily mean most correct we changed the sentence so we now read:

“However, the majority of the studies have pointed to an El Niño-like response following volcanic eruption (for a review of these studies see McGregor et al., 2020).”

365

(McGregor et al., 2020) is a review paper on our understanding of the impact the strong volcanic eruption on ENSO, so the paper itself refers to numerous other studies.

L54: “due to the underlying dynamics of the Pacific Ocean” is vague and does not help the reader to understand this mechanism.

370

We clarified the ocean dynamical thermostat mechanism to make it clearer for the reader:

“due to the preferential cooling of the warm pool in the western Pacific in comparison to the upwelled water in the eastern Pacific.”

375

L66: Do you mean “moves southward”? Usually the ITCZ is fairly centered on the equator.

To avoid confusion, we have changed it to read “southward”

L66: One should give a precise definition of “trade winds”. Also, please provide a clear explanation of how a meridional shift in the ITCZ produces a change in the magnitude of the trade winds, and not just a similar shift in their meridional location. This mechanism is central to the argument but is never given a physical basis.

380

We agree that since the trade winds are a central argument in the ITCZ mechanism this concept require more attention.

We added to the introduction:

“The mechanisms that trigger a change in the ENSO state following volcanic eruptions are still debated. The center of the argument is explaining how a volcanic eruption weaken or amplify the trade winds (i.e. constant surface easterly winds within the tropics).”

385

Regarding how the ITCZ shift produces a change in the magnitude of the trade winds we have added the following sentence in the manuscript:

390

“Trade winds converge towards the ITCZ where their intensity weakens, as the air circulates in an upward direction, creating the so-called doldrums (areas of windless waters). Consequently, a shift of the ITCZ affects the position of the doldrums and the intensity of the trade winds over the equator.

395

L81: “volcano and no-volcano members” won’t be clear to all readers.

We thank the reviewer for bringing this point, why clarified the definition of volcano and no-volcano members:

“Other studies use a small number of ensemble members with volcanic forcing and ensemble members without volcanic forcing starting from different initial conditions ...”

400

L89: The size of eruptions refers to the amount of magma released. Here you are more interested in eruptions that produced the strongest stratospheric aerosol radiative forcing, which is not always the same as being the largest eruption.

We thank the reviewer for pointing this out we now read:

405

“In this study we consider the three largest eruptions, in terms of quantity of aerosols injected in the stratosphere, of the last 100 years; the Agung in Indonesia (8 °S 115 °E) in February 1963; El Chichón in Mexico (17 °N 93 °W) in March 1982; and the Pinatubo in the Philippines (15 °N 120 °E) in June 1991.”

410

L92: The aerosol loading from Pinatubo was *roughly* hemispherically symmetric, but not exactly

We thank the reviewer for pointing this out we changed the phrasing.

L93: The actual hemispheric distribution for Krakatau is quite uncertain, since there are few observations from that time. The forcing used in the simulations is however roughly symmetric.

415

We thank the reviewer for pointing this out we added this nuance.

L103: The relevance of the “total of 600 years of climatology” is not clear.

Thank you for pointing that out we clarified this point in section 2, we now read:

420

“The anomalies calculated are the difference between the reference (3 years before the eruption and for the 200 ensemble members that we refer to as climatology) and periods after the eruption.”

L107: “over-estimate” rather than “amplify” would be more accurate.

425

Thank you for pointing that out.

L115: The source of the aerosol forcing distributions used in these simulations should be given, since it is very important when comparing the results shown here to other studies which use different forcing sets.

We thank the reviewer for this pertinent remark we added in the methodology:

430

“The stratospheric aerosols used in this study are prescribed in the historical simulations of the model (MPI ESM) and comes from the data set of Stenchikov et al. (1998) (Giorgetta et al., 2013).”

L117: I’m not sure we know for sure what processes are most important for controlling the hemispheric asymmetry of the aerosol forcing. Robock (2000) has argued that meteorological conditions at the time of the eruption are important, as it seems winds pushed the Pinatubo SO₂ cloud to the equator. Otherwise, the Pinatubo distribution might have been more NH biased.

435

Thank you for this remark, we added nuance to the statement.

440 **L125: Only 2 forcings are strongly asymmetric.**

Thank you for pointing that out we changed the sentence to :

“The different forcing caused by the three eruptions induces a different cooling of the surface temperature in the two hemispheres (Fig. 4).”

445

Fig 4: x axis label should be more specific (not “year”), and axis extended to include the year of the eruption, with markers at the month of eruption.

We agree that the axis should be extended to see the years of the eruptions. We modified the figure.

450 **L127: the description and Figure are at odds here, as the figure shows a difference in cooling between NH and SH, while the text mostly refers to hemispheric cooling.**

We thank the reviewer for pointing out this inconsistency. What we wanted to say is that if there is a difference of cooling between the NH and the SH it's because one of the two hemispheres has been more cooled than the other and thus, there is a hemispheric cooling of an hemisphere relative to the other hemisphere. To clarify this point we added relative hemispheric cooling in the discussion.

455

L128: the magnitude of the eruptions is less important here than the magnitude of the forcing included in the simulations.

We agree with the reviewer that the amplitude of the eruption in terms of magma ejected is less important than the quantity of stratospheric aerosols. We now read in the results section:

460

“The relative hemispherical cooling associated to Agung (SH) is in absolute values comparable to Pinatubo even if Agung's quantity of aerosols injected in the stratosphere was twice as small (Bluth et al., 1992; Self & Rampino, 2012)”

465 **L131: This statement is not accurate, as strongest cooling seems to occur at the end of year 2.**

We agree that the cooling is not exactly peaking at the beginning of year 2, but it is also not peaking at the end of the year since El Chichón and Pinatubo peak in June. The point is that the maximum cooling and the difference of cooling between the two-hemispheres peak roughly in the same time. We changed the text and we now read:

470 *“The maximum cooling for all three eruptions occurs in the second year and so does the temperature difference between the two hemispheres”.*

L133: Unclear what “results” are referred to. Also, “are consistent with” is quite weak language—with the large amount of fields output by a climate model, one should be able to determine whether the Hadley Cell is displaced or not!

475 We rephrased the sentence with a stronger affirmation:

Precipitation anomalies (Figs. 5 and 6) show the displacement of the Hadley cell associated with the differential cooling between the hemispheres, showing a northward shift of the ITCZ for the eruption of the Agung, and a southward shift for both El Chichón and the Pinatubo, for the three years following the eruption.

480

L134: There is nothing on Fig 5 that looks like a simple shift. On plots of anomalies, a shift should show up as a dipole, with negative and positive anomalies. The anomalies for Agung are almost only negative, while for EC and Pinatubo, the anomaly patterns look more like a narrowing of the ITCZ over the equator.

The dipole pattern is present on figure 5 for the three eruptions: For Agung we can see a small but significant increase of the precipitation north of the ITCZ and a strong reduction of the precipitation south of the ITCZ. Moreover, we can also see the westward winds anomalies associated with the reduction of precipitation, weakening the trade winds and triggering a La Niña-like anomaly via Bjerknes feedback. There is also a similar opposite dipole pattern for El Chichón and Pinatubo in comparison to Agung and it is the main reason why we argue that the ITCZ shift is a dominant mechanism in the ENSO response. Figure 7 also supports that there is a significant northward shift of the ITCZ after Agung and a significant southward shift after El Chichón and Pinatubo.

490

L136: This seems like a rather complicated hypothesis: simpler might be that the response is also sensitive to the magnitude of the forcing, which is stronger for Pinatubo?

We thank the reviewer for the suggestion. We have included it in the text along with the global warming recently proposed hypothesis (Fasullo et al., 2017) that we believe is worth further investigation.

495

“This could indicate that the ITCZ response is sensitive to the magnitude and spatial distribution of the forcing. The on-going global warming could also amplify the rainfall anomaly following the volcanic eruptions through modulation in the ocean stratification and near-surface winds amplifying the response as suggested in a recent study (Fasullo et al., 2017) (Fig. A9).”

500

L210: Nothing presented proves that these mechanisms are completely absent. They can still be active even if another process is more important to the overall response.

We agree with the reviewer, we changed the sentence so we clearly say that it is not that these mechanisms are absent it is just that we can not say that they are dominant since we observe a different response for symmetrical and NH in comparison to SH aerosol distribution. It now reads :

505

“Our work also pointed out that the ODT (Clement et al., 1996), the cooling of the Maritime Continent (Ohba et al., 2013) and of the tropical Africa (Khodri et al., 2017) mechanisms are not dominant for the ENSO response following volcanic eruptions in our model.”

510

L211: A “limited number” of ensemble members is not a drawback per se: there are no studies that use an unlimited number of ensemble members.

We thank the reviewer for pointing that out, we changed the occurrence of limited to small throughout the manuscript.

515 **L212: Why is reliance on statistical tools framed as a limitation of these prior studies?**

The reliance on statistical tools is a limitation as it is based on a small sample of events: for example, Liu et al. (2018) use a synthesis of publicly available proxy-based ENSO reconstructions and two 1500-year long simulations with and without volcanic forcing (no ensemble members). They perform the superposed epoch analysis (SEA) on both proxy data and volcano experiment, concluding that the NH and tropical eruptions lead to El Niño-like conditions in the year following the eruption,

520 while SH eruptions produce a different behavior (La Niña for the proxies; very weak response for the model simulation). The SEA is often used to test whether the El Niño following the eruption is significant or not, using proxy data. However, their SEA analysis show that even before the eruptions there are quite significant NINO3 responses for all eruptions (NH, SH and tropical). It is difficult to determine whether the NINO3 anomalies following the eruptions are induced by the eruptions and hence why we need large ensemble to be able to pull apart the stochastic variability from the volcano signal. To clarify this

525 point we have modified that sentence in the discussion :

“These previous studies that have suggested a different mechanism to explain the ENSO response to volcanic eruptions are based on a small number of ensemble members (e.g. 5 members for 3 eruptions for the SH plume in Zuo et al. (2018)) or they heavily rely on statistical tools using a small sample of events (e.g. SEA in Liu et al. (2018))”

530

References

- Bjerknes, J. (1969). Monthly Weather Review Atmospheric Teleconnections From the Equatorial Pacific. *Monthly Weather Review*.
- Colose, C. M., LeGrande, A. N., & Vuille, M. (2016a). Hemispherically asymmetric volcanic forcing of tropical hydroclimate during the last millennium. *Earth System Dynamics*. <https://doi.org/10.5194/esd-7-681-2016>
- 535 Giorgetta, M. A., Jungclaus, J., Reick, C. H., Legutke, S., Bader, J., Böttinger, M., et al. (2013). Climate and carbon cycle changes from 1850 to 2100 in MPI-ESM simulations for the Coupled Model Intercomparison Project phase 5. *Journal of Advances in Modeling Earth Systems*. <https://doi.org/10.1002/jame.20038>
- Kang, S. M., Held, I. M., Frierson, D. M. W., & Zhao, M. (2008). The response of the ITCZ to extratropical thermal forcing: Idealized slab-ocean experiments with a GCM. *Journal of Climate*. <https://doi.org/10.1175/2007JCLI2146.1>
- 540 Khodri, M., Izumo, T., Vialard, J., Janicot, S., Cassou, C., Lengaigne, M., et al. (2017). Tropical explosive volcanic eruptions can trigger El Niño by cooling tropical Africa. *Nature Communications*. <https://doi.org/10.1038/s41467-017-00755-6>
- Liu, F., Li, J., Wang, B., Liu, J., Li, T., Huang, G., & Wang, Z. (2018). Divergent El Niño responses to volcanic eruptions at different latitudes over the past millennium. *Climate Dynamics*. <https://doi.org/10.1007/s00382-017-3846-z>
- 545 Maher, N., McGregor, S., England, M. H., & Gupta, A. Sen. (2015). Effects of volcanism on tropical variability. *Geophysical Research Letters*. <https://doi.org/10.1002/2015GL064751>
- McGregor, S., Khodri, M., Maher, N., Ohba, M., Pausata, F. S. R., & Stevenson, S. (2020). The Effect of Strong Volcanic Eruptions on ENSO. <https://doi.org/10.1002/9781119548164.ch12>
- 550 Milinski, S., Maher, N., & Olonscheck, D. (2019). How large does a large ensemble need to be? *Earth System Dynamics Discussions*. <https://doi.org/10.5194/esd-2019-70>
- Pausata, F. S. R., Grini, A., Caballero, R., Hannachi, A., & Seland, Ø. (2015). High-latitude volcanic eruptions in the Norwegian Earth System Model: The effect of different initial conditions and of the ensemble size. *Tellus, Series B: Chemical and Physical Meteorology*. <https://doi.org/10.3402/tellusb.v67.26728>
- 555 Schneider, T., Bischoff, T., & Haug, G. H. (2014). Migrations and dynamics of the intertropical convergence zone. *Nature*. <https://doi.org/10.1038/nature13636>
- Stechmann, S. N., & Ogrosky, H. R. (2014). The Walker circulation, diabatic heating, and outgoing longwave radiation. *Geophysical Research Letters*. <https://doi.org/10.1002/2014GL062257>
- Stevenson, S., Otto-Bliesner, B., Fasullo, J., & Brady, E. (2016). “El Niño Like” hydroclimate responses to last millennium volcanic eruptions. *Journal of Climate*. <https://doi.org/10.1175/JCLI-D-15-0239.1>
- 560 Zuo, M., Man, W., Zhou, T., & Guo, Z. (2018). Different impacts of Northern, tropical, and Southern volcanic eruptions on the tropical pacific SST in the Last Millennium. *Journal of Climate*. <https://doi.org/10.1175/JCLI-D-17-0571.1>

The sensitivity of the ENSO to volcanic aerosol spatial distribution in the MPI Grand Ensemble

Benjamin Ward¹, Francesco S.R. Pausat¹, Nicola Maher²

¹ Department of Earth and Atmospheric Sciences, University of Quebec in Montreal, Montreal, Canada

5 ² Max-Planck-Institute for Meteorology, Hamburg, Germany

Correspondence to: Benjamin Ward (ward_soucy.benjamin@courrier.uqam.ca)

Abstract. Using the Max Planck Institute Grand Ensemble (MPI-GE) with 200 members for the historical simulation (1850-2005), we investigate the impact of the spatial distribution of volcanic aerosols on the ENSO response. In particular, we select 3 eruptions (El Chichón, Agung and Pinatubo) in which the aerosol is respectively confined to the Northern Hemisphere, the Southern Hemisphere or equally distributed across the equator. Our results show that **relative** ENSO anomalies start at the end of the year of the eruption and peak the following one. Especially, we found that when the aerosol is located in the Northern Hemisphere or is symmetrically distributed, **relative** El Niño-like anomalies develop while aerosol distribution confined to the Southern Hemisphere leads to a **relative** La Niña-like anomaly. Our results strongly point to the volcanically induced displacement of the ITCZ as the main mechanism that drives the ENSO response, while suggesting that the other mechanisms (the ocean dynamical thermostat, the cooling of tropical northern Africa or of the Maritime continent) commonly invoked to explain the post-eruption ENSO response appear not to be at play in our model.

1 Introduction

Aerosol particles from volcanic eruptions **are one of the most important** non-anthropogenic radiative forcing that have influenced the climate system in the past centuries (Robock, 2000). Oxidised, sulfur gases (mainly in form of SO_2) injected into the stratosphere by large Plinian eruptions form sulfate aerosols (H_2SO_4) (Pinto et al., 1989; Pollack et al., 1976) that have a time residence of 1-3 years (Barnes & Hofmann, 1997; Robock & Yuhe Liu, 1994). These particles both scatter and absorb incoming solar radiation as well as part of the outgoing longwave radiation (Stenchikov et al., 1998; Timmreck, 2012). For intense and sulfur-rich volcanic eruptions, the net effect is a general cooling of the surface and a warming in the stratosphere where the aerosols tend to reside longer (Harshvardhan, 1979; Rampino & Self, 1984). The maximum global cooling **seen in modeling studies is generally reached** within 6-8 months following the eruption peak in optical depth before returning to normal values after about 3 to 4 years (Thompson et al., 2009). These rapid modifications in temperature **may** induce dynamical changes in the atmosphere and in the ocean including a strengthening of the polar vortex (e.g., Christiansen, 2008; Driscoll et al., 2012; Kodera, 1994; Stenchikov et al., 2006), a weakening in the African and Indian Monsoon (e.g. Iles et al., 2013; Man et al., 2014; **Paik et al., 2020**; Trenberth & Dai, 2007; Zambri & Robock, 2016) as well as forced changes on the El Niño-Southern Oscillation (ENSO) (e.g., Emile-Geay et al., 2008; McGregor & Timmermann, 2011; Pausat et al., 2015; Wang et al., 2018).

Paleoclimate archives and observations from the past centuries suggested that large tropical eruptions are usually followed by a warm sea-surface temperature (SST) anomaly in the Pacific (e.g., Adams et al. , 2003; D'Arrigo et al. , 2005; Li et al., 2013; S. McGregor et al. , 2010; Wilson et al., 2010) **even if there is still uncertainty on the significance of these results (Dee et al., 2020). In addition,** El Niño events followed in the first or the second winter after the five largest eruptions of the last 150 years (**Krakatau** in August 1883, Santa Maria in October 1902, Agung in **February** 1963, El Chichón in **March** 1982 and Pinatubo in June 1991). However, the Santa Maria, El Chichón and Pinatubo eruptions occurred after an El Niño event was already developing making it difficult to determine a causal link between ENSO and these eruptions (e.g., Self et al., 1997; Nicholls, 1988).

Moreover, modelling studies initially found divergent responses for the ENSO changes after large tropical eruptions (Ding et al., 2014; McGregor & Timmermann, 2011; Stenchikov et al., 2006; Zanchettin et al., 2012). However, the majority of the studies have pointed to an El Niño-like response following volcanic eruption (**for a review of these studies see McGregor et al., 2020**). In particular, the use of relative sea surface temperature (RSST) or sea surface height (SSH) instead of SST have helped to disentangle the ENSO response from volcanically induced cooling in the Pacific and to highlight the dynamical ENSO response (Khodri et al., 2017; Maher et al., 2015).

Although a consensus is emerging, different aerosol spatial distributions may give rise to different ENSO responses. Stevenson et al., (2016) investigated the impact of NH, SH and tropical volcanic eruptions using the Community Earth System Model (CESM 1.1) Last Millennium Ensemble. They concluded that while NH and tropical eruptions tend to favour El Niño-like conditions, SH eruptions enhance the probability of La Niña events within one year following the eruptions. Conversely, Liu, Li, et al., (2018) through a millennium simulation performed with CESM 1.0 and Zuo et al., (2018) using the Community Earth System Model Last Millennium Ensemble (CESM-LME) concluded that SH, NH and tropical eruptions all resulted in El Niño-like conditions in the second year after the eruption. **The terms El Niño-like and La Niña-like conditions are used in the context of modeling studies to describe an anomalous warming or cooling of the equatorial Pacific relative to the reference case.**

The mechanisms that trigger a change in the ENSO state following volcanic eruptions are still debated. The center of the argument is explaining how a volcanic eruption weaken or amplify the trade winds (i.e. constant surface eastward winds within the tropics). One of the most frequently used hypotheses is the “ocean dynamical thermostat” mechanism (ODT) (Clement et al., 1996), where a preferential cooling in the western Pacific relative to the eastern Pacific takes place **due to the preferential cooling of the warm pool in the western Pacific in comparison to the upwelled water in the eastern Pacific.** Such a differential cooling weakens the zonal SST gradient along the equatorial Pacific which causes a relaxation of the trade winds, leading to a temporary weakening of the ocean upwelling in the eastern Pacific. This process is then amplified by the Bjerknes feedback, yielding an El Niño (Bjerknes, 1969). A related mechanism for the preferential El Niño anomalies following volcanic eruptions is based on the recharge-discharge theory of ENSO, including changes in the wind stress curl during the eruption year as one of the triggering factors (McGregor & Timmermann, 2011; Stevenson et al. 2017). However,

through a set of sensitivity experiments, Pausata et al., (2020) have questioned the existence of the ODT mechanism in coupled climate models following volcanic eruptions, pointing to the Intertropical convergence zone (ITCZ) displacement and extratropic-to-tropic teleconnections as key mechanisms in affecting post-eruption ENSO. The ITCZ-shift mechanism was originally proposed for the ENSO response to high-latitude eruptions (Pausata et al., 2015; 2016) and then suggested to also
70 be at work for tropical asymmetric eruptions (Colose et al., 2016; Stevenson et al., 2016). **Trade winds converge towards the ITCZ where their intensity weakens, as the air circulates in an upward direction, creating the so-called doldrums (areas of windless waters). Consequently, a shift of the ITCZ affects the position of the doldrums and the intensity of the trade winds over the equator.** In general, the ITCZ shift away from the hemisphere that is cooled (Kang et al., 2008; Schneider et al., 2014). Consequently, for an eruption with aerosol concentrated in the NH, the ITCZ location moves
75 equatorward, weakening the trade winds and leading to an El Niño-like anomaly via the Bjerknes feedback (Bjerknes, 1969). In contrast, the ITCZ moves northward following a larger SH cooling, strengthening the trade winds and triggering La Niña-like anomalies as seen in Colose et al. (2016) and Stevenson et al. (2016). Khodri et al. (2017) have invoked atmospheric teleconnections associated with the volcanically induced cooling of tropical Africa and weakening of the West African monsoon, **which favours anomalous Rossby and Kelvin waves. These anomalous waves** alter the Walker circulation and
80 **were identified as** the primary cause of the post-eruption El Niño-like anomalies. A similar mechanism has been suggested based on the cooling of the Maritime continent or south-eastern Asia instead of tropical Africa (Eddebbbar et al., 2019; Ohba et al., 2013; Predybaylo et al., 2017). However, there is yet no consensus as to which of these proposed mechanisms is the main driver of the ENSO response after large volcanic eruptions.

Modeling studies have investigated the impact of volcanic eruptions on ENSO using different approaches. Many studies have
85 used a superposed epoch (SEA) or composite analysis, in which they used a window of a few years before the eruption to create a reference to compare with the post-eruption period (e.g. Liu, Li, et al., 2018; Zuo et al., 2018). The significance of the response to volcanic eruptions is then assessed using a Monte Carlo method. However, this statistical methodology has some shortcomings as it is not able to fully remove the signal of internal variability: ENSO anomalies can still be seen in the reference period (see for example figure 4 in Liu, Li, et al., (2018)). Other studies use a **small** number of ensemble members **with**
90 **volcanic forcing** and **ensemble members without volcanic forcing** starting from different initial conditions (e.g. McGregor & Timmermann, 2011; Predybaylo et al., 2017; Sun et al., 2019). However, when starting the two ensemble sets from different initial conditions, a large number of ensemble members (equivalent to at least 150 years reference period/climatology) is needed to isolate the internal variability of ENSO (Milinski et al., 2019; Wittenberg, 2009). Here, for the first time, we use a
95 200-member ensemble taken from the Max Planck Institute Grand Ensemble (MPI-GE) for the historical simulations (1850-2005) (Maher et al., 2019) to investigate the ENSO response to hemispherically symmetric and asymmetric volcanic eruptions. The large ensemble and the different aerosol distributions allow us to shed light on the mechanisms at play in altering the ENSO state after volcanic eruptions.

2 Methodology and Experimental Design

In this study we consider the three largest eruptions, **in terms of quantity of aerosols injected in the stratosphere**, of the last 100 years; the Agung in Indonesia (8 °S 115 °E) in February 1963; El Chichón in Mexico (17 °N 93 °W) in March 1982; and the Pinatubo in the Philippines (15 °N 120 °E) in June 1991. Two eruptions have an asymmetrical aerosol distribution, so either the aerosols are confined to the NH (El Chichón) or to the SH (Agung). The Pinatubo eruption has an **approximately** symmetrical distribution with the sulfate aerosols spread across both hemispheres. We also considered the eruption of the **Krakatau** in Indonesia (6 °S 105 °E) in 1883 **which is also modelled** with an **approximately** symmetrical aerosol plume to further corroborate our results. For clarity, we only show the results for Pinatubo, which are qualitatively similar to **Krakatau**. The results of **Krakatau** are displayed in the supplementary material (Figs. A7, A8 and A9). **The stratospheric aerosols used in this study are prescribed in the historical simulations of the model (MPI ESM) from the data set of Stenchikov et al. (1998) (Giorgetta et al., 2013).**

We use 200 ensemble members of the historical simulations (1850-2005) performed using the Max Planck Institute for Meteorology Earth System Model 1.1 (MPI-ESM 1.1) (Giorgetta et al., 2013) as part of the Max Planck Institute Grand Ensemble (Maher et al., 2019). Such a large ensemble also allows us to analyse the ENSO response of individual eruptions instead of a composite of multiple eruptions as done in previous studies that used a **small** number of ensembles (e.g. Maher et al., 2015; Stevenson et al., 2016; Zuo et al., 2018). All the ensemble members are initialized from different years of a long preindustrial control run (2000 years) after it has reached a quasi-stationarity state. The model horizontal resolution is roughly 1.8° for the atmosphere and 1.5° for the ocean with 16 vertical levels for both the atmosphere and the ocean.

The anomalies calculated are the difference between the reference (3 years before the eruption and for the 200 ensembles members that we refer to as climatology) and periods after the eruption. A Student t-test is used to estimate the significance of the mean changes before and after the eruptions at the 95% confidence level.

Large tropical eruptions induce a global cooling so that El-Niño response may be partly masked, and the La-Niña response amplified (Maher et al., 2015). Furthermore, some climate models **overestimate** the volcanically induced cooling (e.g. Anchukaitis et al., 2012; Stoffel et al., 2015). To better highlight the dynamical changes, we remove the tropical SST mean from the original SST, this is known as the relative sea surface temperature (RSST) (Vecchi & Soden, 2007). In this study, we use the RSST to isolate the intrinsic ENSO signal (Khodri et al., 2017).

3.1 ENSO response and its link to the ITZC-shift mechanism

The volcanic eruptions analyzed in the present study show three distinct aerosol plumes. While the aerosol distribution from the Pinatubo eruption is symmetrical around the equator, Agung and El Chichón eruptions both created to a large extent confined distribution in respectively the SH and the NH (Fig. 1). For the Pinatubo and El Chichón the aerosol optical depth peaks in the winter that follows the eruptions. For the Agung this maximum is reached in the winter of the second year after the eruption. **The reasons why similar eruptions can lead to different aerosol distributions are still being investigated, but some causes are** the location of the volcanoes, the season and the strength of the eruption (Stoffel et al., 2015; Toohey et al., 2011).

Our simulations show a **relative** El Niño-like response to the El Chichón and Pinatubo eruptions and a **relative** La Niña-like response to the Agung eruption (Figs. 2 and 3). **The relative** ENSO anomalies develop at the beginning of the year after the eruption (Year 2) and then peak that boreal winter for El Chichón and Pinatubo or in the third boreal winter for Agung. The westerly anomalies in the trade winds are detected starting in the autumn of the eruption (Year 1). For all the eruptions, the relative Niño 3.4 index peaks in the winter of the year after the eruption reaching a maximum of approximately +0.3 °C for El Chichón and the Pinatubo and a minimum of -0.2 °C for Agung (Fig. A3). **The results using the SST (Figs. A11, A12 and A13) are qualitatively similar to the RSST (Figs. 2, 3, and A3), but the El Niño-like anomalies are less strong since they are partially masked by the global cooling induced by the stratospheric aerosols which is in agreement with other studies (Khodri et al., 2017; Maher et al., 2015).**

Furthermore, the temperature anomalies following the Agung eruption are not just superficial but extend down to 200 m depth (Fig. A14). The warming below 100 m in the western Pacific and the cooling along the thermocline in the eastern side of the basin are typical of an ongoing La Niña : the pattern is indeed remarkably similar to a composite of La Niña events occurring in the reference periods before the three eruptions (Fig. A17). On the other hand, the temperature anomalies for the El Chichón and Pinatubo eruptions show opposite results as expected under El Niño conditions (Figs. A15 and A16). Moreover, the wind anomalies following Agung (see Fig. 2 and 3) are opposite compared to El Chichón , hence leading to opposite upwelling conditions along the equator, further corroborating that the ocean temperature anomalies are mostly dynamically driven through the Bjerknes feedback (Bjerknes, 1969). The different forcing caused by the three eruptions induces a different cooling of the surface temperature in the two hemispheres (Fig. 4). Although Pinatubo is the most intense eruption and has the largest global temperature decrease (Fig. A2), El Chichón shows the strongest hemispherical cooling (Fig. 4). The relative hemispherical cooling associated to Agung (SH) is in absolute values comparable to Pinatubo even if Agung's quantity of aerosols injected in the stratosphere was twice as small (Bluth et al., 1992; Self & Rampino, 2012). Furthermore, while the aerosol distribution of the Pinatubo eruption is symmetric, the relative cooling is not and is concentrated in the NH, which is likely due to uneven distribution of landmass between hemispheres (i.e.

reduced heat capacity in the NH). The maximum cooling for all three eruptions occurs **in the second year** and so does the temperature difference between the two hemispheres (Figs. 4 and A1).

Precipitation anomalies (Figs. 5 and 6) show the displacement of the Hadley cell associated with the differential cooling between the hemispheres, showing a northward shift of the ITCZ for the eruption of the Agung, and a southward shift for both El Chichón and the Pinatubo, for the three years following the eruption. Additionally, the Pinatubo's rainfall anomaly is the largest even though the difference in the cooling of each hemisphere is stronger for El Chichón. This could indicate that the **ITCZ response is sensitive to the magnitude and spatial distribution of the forcing**. The on-going global warming could also amplify the rainfall anomaly following the volcanic eruptions through modulation in the ocean stratification and near-surface winds amplifying the response as suggested in a recent study (Fasullo et al., 2017) (Fig. A9). **Moreover, the precipitation asymmetry index (PAi) (Colose et al., 2016) further highlight the ITCZ shift and weakening (Fig. 7). The expression for the PAi is given by:**

$$PAi = \frac{P_{20^{\circ}N-10^{\circ}N} - P_{10^{\circ}N-Eq}}{P_{20^{\circ}N-Eq}}$$

It represents the variation of the zonal precipitation around the average climatological mean of the ITCZ in our model, which is roughly 10 °N. In figure 7, the positive variation of the PAi after Agung eruption means a northward shift of the ITCZ and the negative variations of the PAi after Pinatubo and El Chichón eruptions means a southward shift of the ITCZ. We find that the ITCZ displacement and associated rainfall anomalies peak the second year after the eruption, when the differential cooling of the hemisphere is larger (Figs. 4, 5, 6 and 7). The ITCZ displacement is associated with a strengthening of the trade winds for the Agung eruption and a weakening for the El Chichón and Pinatubo eruptions as expected by the direction of the ITCZ movement in each case. These wind anomalies affect then the ENSO state: a change in the strength of the trade winds along the equatorial Pacific alters the ocean upwelling in the eastern side. This leads to a change in the east-west temperature contrast across the tropical Pacific, which is amplified by the Bjerknes feedback (Bjerknes, 1969) thus altering the ENSO state. All our results (the evolution of the **relative** Niño 3.4 index, the precipitation anomalies or the **relative** temperature anomalies) show an almost perfect symmetry between the tropical/NH distribution and the SH distribution (Figs. 2, 3, 4, 5, 6 and A2), which strongly suggests that the volcanically induced ITCZ displacement is the key mechanism to explain the ENSO response to the volcanic forcing in agreement with others studies (Colose et al., 2016; Pausata, et al., 2016; Stevenson et al., 2016; Pausata et al., 2020).

3.2 ENSO response and its link to other mechanisms

The most commonly invoked mechanism that explains the ENSO response after large tropical volcanic eruptions is the ODT (Clement et al., 1996) and the preferential cooling of the warm pool relative to the eastern equatorial Pacific, leading to an El Niño-like response (e.g. Emile-Geay et al., 2008; Mann et al., 2005). However, in our simulations even if there is a volcanic aerosol over the equatorial Pacific and a surface cooling for all the eruptions (Figs. 1, A3, A4 and A5), we see a negative phase

of **the relative** ENSO and an anomalous easterly wind stress developing after the Agung eruption (Figs. 2 and 3). These results thus suggest that the ODT is not a dominant mechanism in our model.

190 Another mechanism often used to explain the post-eruption El Niño-like response is related to the cooling of the Maritime
Continent first proposed by Ohba et al. (2013) and also suggested in recent studies (e.g., Eddebbbar et al., 2019) : the smaller
heat capacity of the land in comparison to the ocean cause a stronger land cooling that reduces the temperature gradient between
the Maritime Continent and the western Pacific Ocean. Such temperature changes lead to a weakening of the trade winds and
an eastward shift of the rainfall (El Niño pattern). Our results show a cooling of the Maritime Continent and a reduction of the
195 convective activity in the three eruptions (Figs. A3, A4 and A5). Nevertheless, our model simulates the development of a
relative La Niña-like conditions after the eruption of the Agung (Figs. 1 and 2), which is at odds with the cooling of the
Maritime Continent mechanism where **relative** El Niño-like conditions would be expected for all three eruptions.

Khodri et al., (2017) suggested that the cooling of tropical Africa, following volcanic eruptions, may increase the likelihood
of an El Niño events through the weakening of the West African Monsoon and changes in the Walker circulation. **More**
200 **specifically, the reduction of the tropical precipitation and tropospheric cooling favours anomalous atmospheric Rossby
and Kelvin waves in autumn (SON), with a weakening of the trade winds over the western Pacific, leading to El Niño-
like conditions in the year after the eruption.** Our results show a mixed response over Africa with Agung and Pinatubo both
displaying a cooling (Figs. A3 and A5) but leading to different **relative** ENSO responses (Figs. 1 and 2). Moreover, after El
Chichón eruption a warming of the tropical northern Africa takes place in the first year and an El Niño-like anomaly develops
205 (Figs. 2, 3 and A4). Hence, in our model, the volcanically induced cooling of tropical Africa and the atmospheric perturbations
associated with the suppression of the African monsoon seem not to play a critical role in altering the ENSO state following
volcanic eruptions.

Recently, Pausata et al., (2020) proposed an additional mechanism related to the extratropical-to-tropical teleconnections that
tends to favour an El Niño-like response for both NH and SH eruptions, hence playing in synergy (NH eruptions) or against
210 (SH eruptions) the ITCZ-shift mechanism. However, our qualitative analysis of the sea level pressure (SLP) anomalies does
not match the changes expected by this mechanism (cf. Fig. A10 to Fig. 4 (a-d) in Pausata et al., (2020)). In this recent study,
the volcanic aerosol alters the meridional temperature gradient of the atmosphere that eventually causes a poleward shift of
the Pacific jet stream and a strong cyclonic surface pressure anomaly over the midlatitude to subtropical Pacific basin in both
NH and SH eruptions in the first summer following the eruptions. In our simulation, the response is opposite for the Agung
215 and El Chichón or Pinatubo eruptions, suggesting more that the simulated extratropical anomalies are induced by the **relative**
ENSO changes due to the eruption rather than affecting ENSO (Fig. A10). The reason of the disagreement could lie in the fact
that the El Niño/La Niña-like response following the volcanic eruptions peak in the first winter in Pausata et al., (2020)
modeling study, while in our model in the second winter (Figs. 2 and 3). The extratropical-to-tropical teleconnection could
make the El Niño development following NH/symmetric eruptions occur faster than in our case where such a teleconnection
220 appears not to be present. Ad hoc sensitivity experiments are necessary to rule out the above-mentioned mechanisms in our
model.

4 Discussion and conclusions

Our study used the largest ensemble simulation (200 ensembles) currently available of the historical period performed with the MPI-ESM model to better understand the impact of the volcanic eruptions on ENSO. Our results strongly point to the volcanically induced ITCZ displacement as the primary driver of the ENSO response following volcanic eruptions. In our simulations, the ENSO response after the eruptions critically depends on the distribution of the aerosol plume. When the volcanic aerosol distribution is confined to the NH or its distribution is symmetrical across the hemispheres the ENSO state tends towards a positive phase (**relative** El-Niño like conditions ; Fig. 2 (d-i)), while when the aerosols are confined to the SH the ENSO state is pushed towards a negative phase (**relative** La Niña-like conditions ; Figs. 2 (a-c)). The displacement of the ITCZ following the eruptions, caused by the asymmetric cooling of the hemisphere that pushes the ITCZ towards the hemisphere that is less cooled (Kang et al., 2008; Schneider et al., 2014). Both the eruptions with aerosol confined to the NH and symmetrically distributed across the hemispheres preferentially cool the NH, consequently shifting the ITCZ southwards, weakening the trade winds over the equatorial Pacific and triggering El Niño like response through the Bjerknes feedback (Bjerknes, 1969). The eruption with the aerosol plume confined to the SH instead cools exclusively the SH, pushing the ITCZ northward and strengthening the trade winds, leading to La Niña-like response (Figs. 5, 6 and 7).

The ITCZ mechanism we see at play in our model is supported by other recent studies performed with different climate models (Pausata,et al., 2015, 2020; Stevenson et al., 2016; Colose et al., 2016). Pausata et al. (2020) through a set of sensitivity experiments in which the volcanic aerosol forcing is confined to either the northern or the southern hemisphere show the key role of the ITCZ displacement in driving the ENSO response. They also highlighted the presence of another mechanism related to the extratropical-to-tropical teleconnections that no matter the type of eruption (NH or SH) tends to favour an El-Niño like response. Hence, it plays in synergy (NH eruptions) or against (SH eruptions) the ITCZ-shift mechanism. However, the simulated SLP changes in the extratropics in our model seem to be in response to the volcanically induced ENSO changes rather than affecting the ENSO response (cf. Fig. A10 to Fig. 4 (a-d) in Pausata et al., (2020)).

Our work also pointed out that the ODT (Clement et al., 1996), the cooling of the Maritime Continent (Ohba et al., 2013) and of the tropical Africa (Khodri et al., 2017) mechanisms **are not dominant for the ENSO response. These previous studies that have suggested a different mechanism to explain the ENSO response to volcanic eruptions are based on a small number of ensemble members (e.g. 5 members for 3 eruptions for the SH plume in Zuo et al. (2018)) or they heavily rely on statistical tools using a small sample of events (e.g. SEA in Liu et al. (2018))**. Consequently, those results may be biased by the use of a restrained number of ensemble members. Hence, our study points out the importance of a large number of ensemble members when investigating the ENSO response to volcanic eruptions. The absence of these mechanisms following volcanic eruptions is also in qualitative agreement with the modeling experiments in Pausata et al. (2020).

Finally, our results are consistent with the predominance of post-eruption El Niño events ((Adams et al., 2003; McGregor et al., 2020) and it can provide an explanation on why the majority of both observations and reconstructions are displaying El Niño events instead of La Niña events. However, the ENSO responses discussed in this study are only tendential (El Niño-like

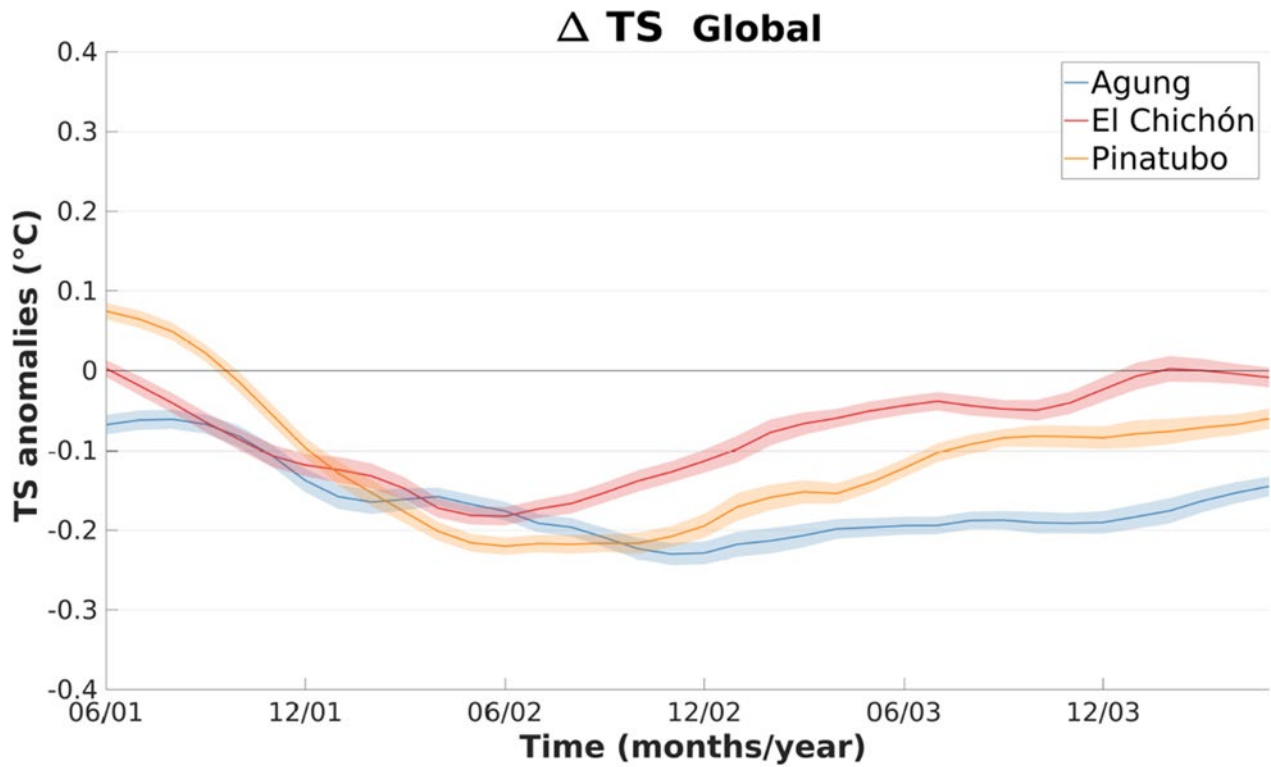
255 or La Niña-like response), i.e., intrinsic variability evolving toward a La Niña at the time of the eruption would not necessarily
lead to a post-eruption El Niño event even for a NH or symmetrical eruption, but rather to a dampening of the ongoing La
Niña. **Furthermore, our model suggests the peak in ENSO anomalies to be in the second or third year after the eruption
similar to most modeling studies (Khodri et al., 2017; Lim et al., 2016; McGregor & Timmermann, 2011; Ohba et al.,
2013; Stevenson et al., 2017). This is at odds with the reconstructions and observations that see a peak in ENSO
260 anomalies in the first winter following the eruption (McGregor et al., 2010; 2020) and possibly extending to the second
year (Adams et al., 2003). The delayed ENSO response in our model simulations relative to reconstructions and
observations may be related to the apparent lack of extratropical-to-tropical teleconnections (Pausata et al., 2020) that
could favour El Niño-like response already on the first winter following the eruption or other biases within the climate
models (e.g., double ITCZ).**

265

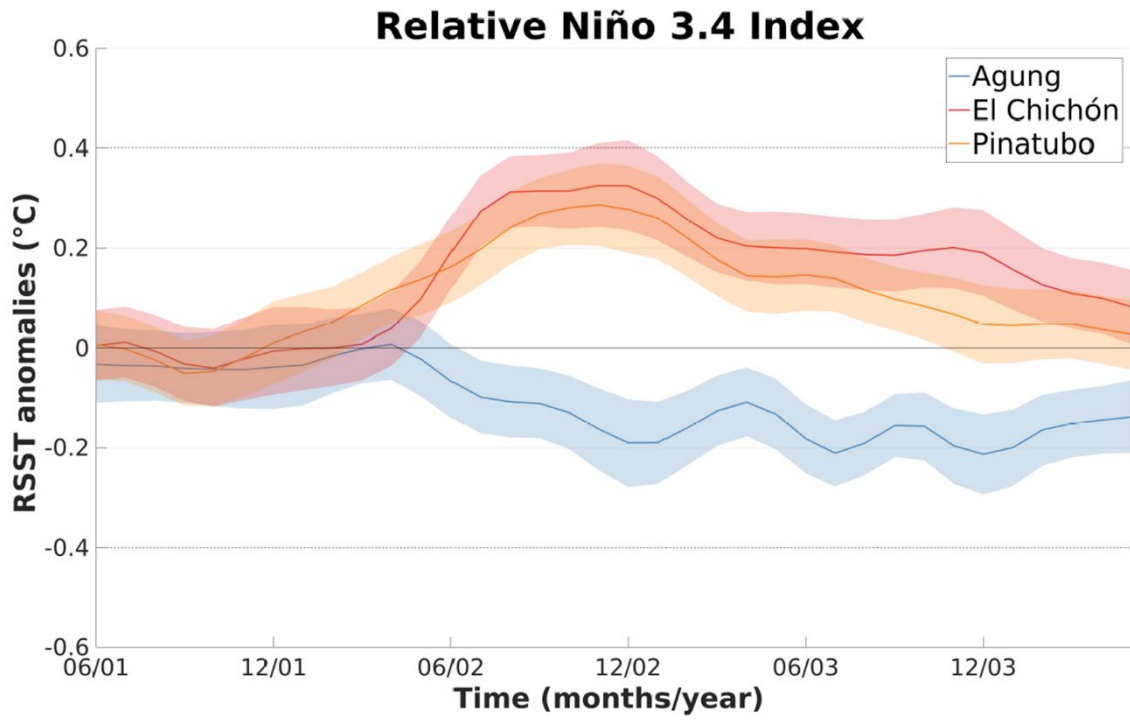
In conclusion, our results provide further insights into the mechanism driving the ENSO response to volcanic eruptions,
highlighting in particular the role of the ITCZ shift. However, further coordinated efforts with specific sensitivity studies are
necessary to delve into the other proposed mechanisms and to unravel the difference between modeling studies and
reconstructions with regards to the peak of the ENSO response. Given that ENSO is the major leading mode of tropical climate
270 variability, which has worldwide impacts, these types of studies are also necessary to help improve seasonal forecasts following
large volcanic eruptions.

Appendices

Appendix A



275 **Figure A1.** Evolution of the ensemble mean of the global the cooling in the three eruptions case for three years, starting at the first summer after the eruption. The 3-year climatology is subtracted to calculate the anomalies. Shading represents twice the standard error of the ensemble mean (i.e. 95% confidence interval).



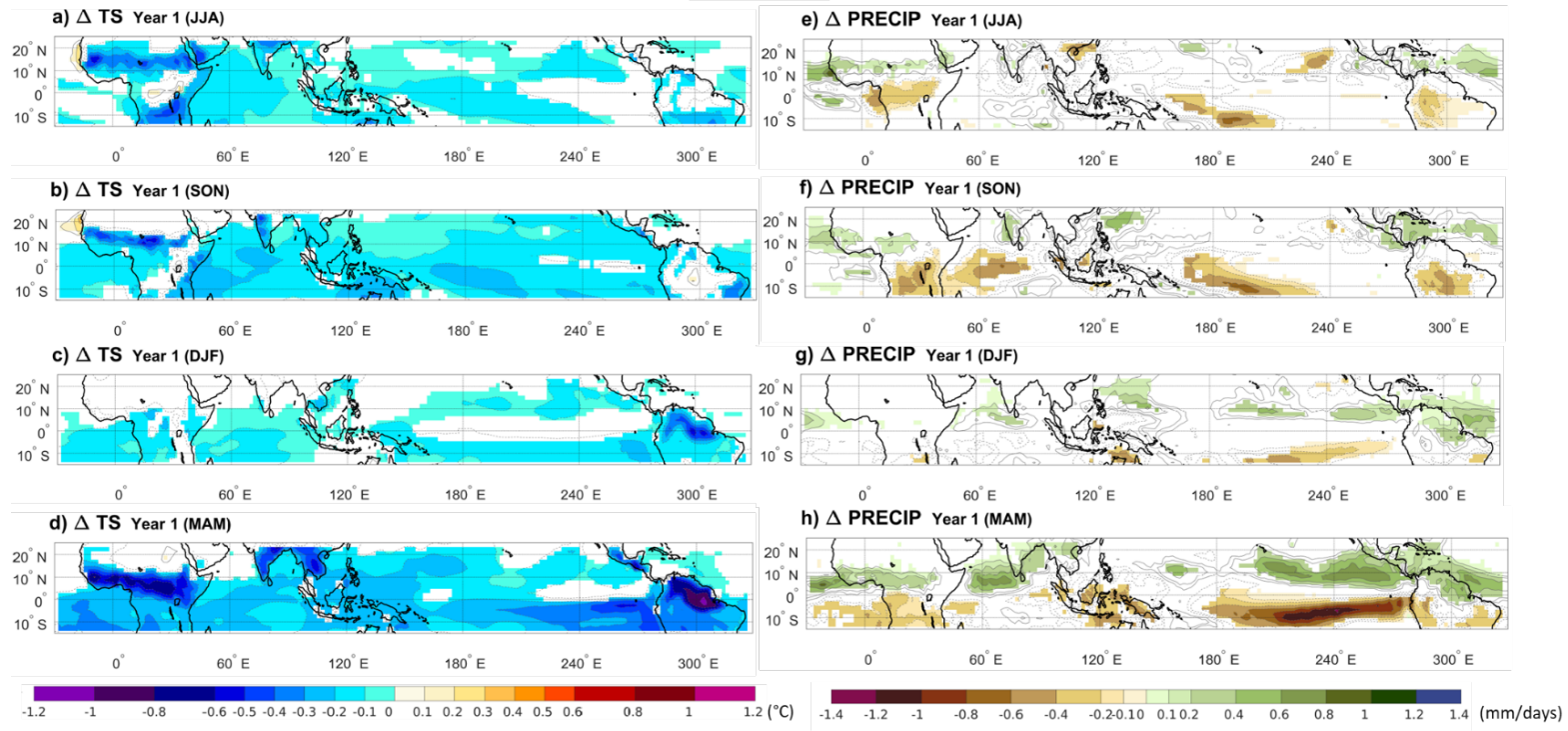
280 **Figure A2.** Ensemble mean changes in the relative Niño 3.4 index after each eruption. The 3-year climatology is subtracted to calculate the anomalies. Shading represent twice the standard error of the mean using an approximate 95% confidence interval.

285

290

295

Agung



300 **Figure A3.** Ensemble mean of changes in surface temperature (a,b,c,d) and precipitation (e,f,g,h) between the climatology and the volcano case for each seasons of the year after Agung eruption. Only significant anomalies are showed with an approximate 95% confidence level using a Student *t*-test. Contour shows temperature and precipitations anomalies following the color bar scale (solid line for positive anomalies and dashed line for negative anomalies).

305

310

315

El Chichón

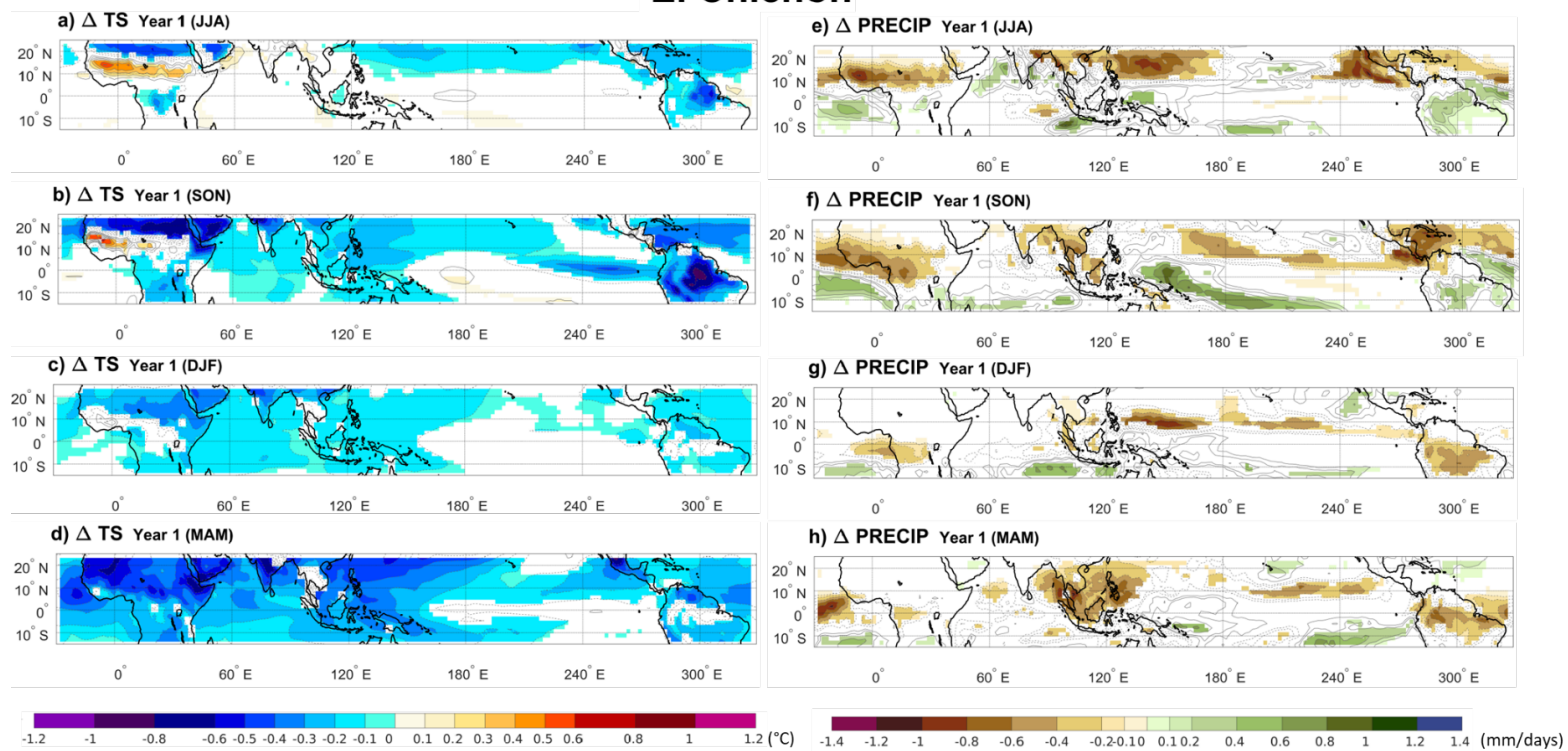
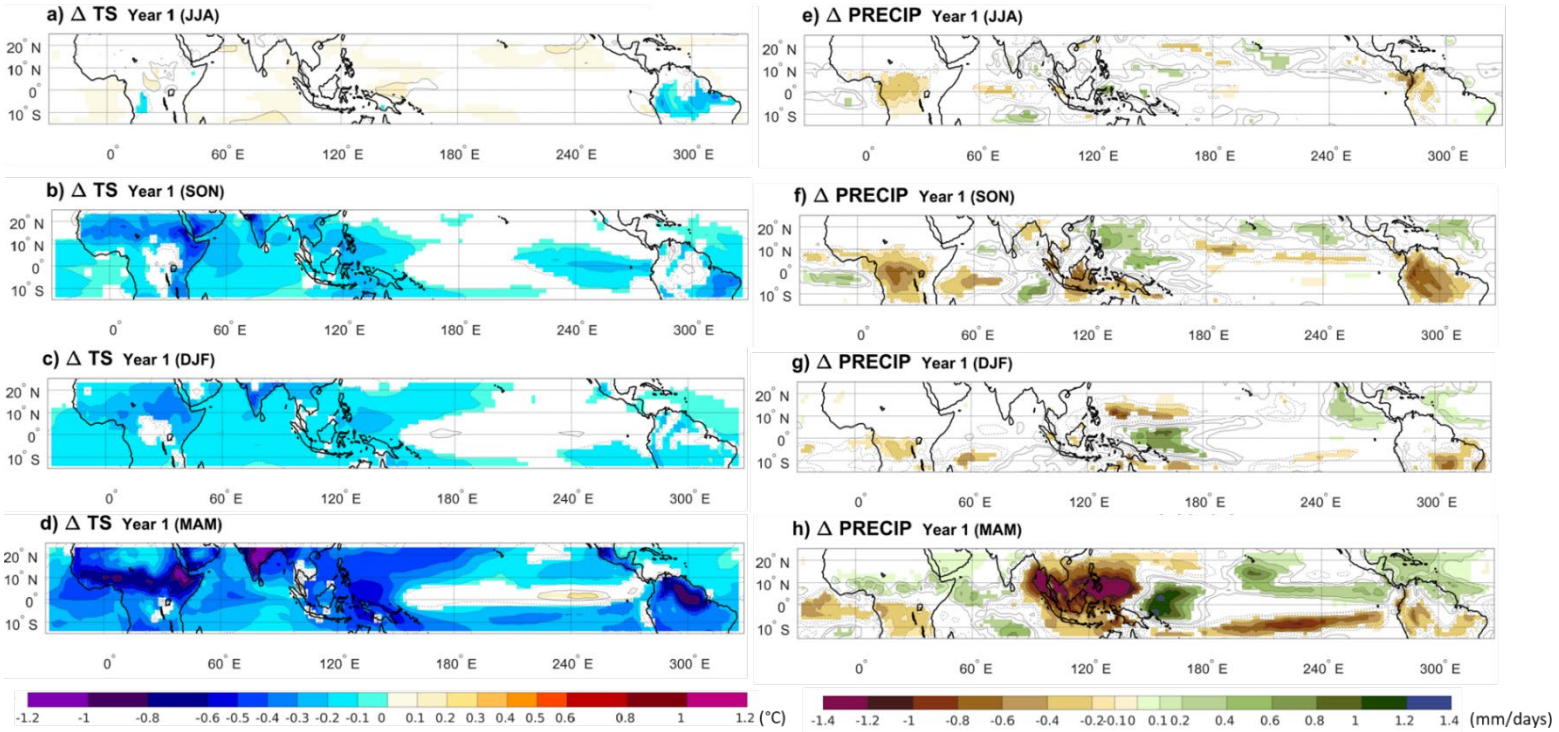


Figure A4. Ensemble mean of changes in surface temperature (a,b,c,d) and precipitation (e,f,g,h) between the climatology and the volcano case for each seasons of the year after El Chichón eruption. Only significant anomalies are showed with an approximate 95% confidence level using a Student *t*-test. Contour shows temperature and precipitations anomalies following the color bar scale (solid line for positive anomalies and dashed line for negative anomalies).

325

330

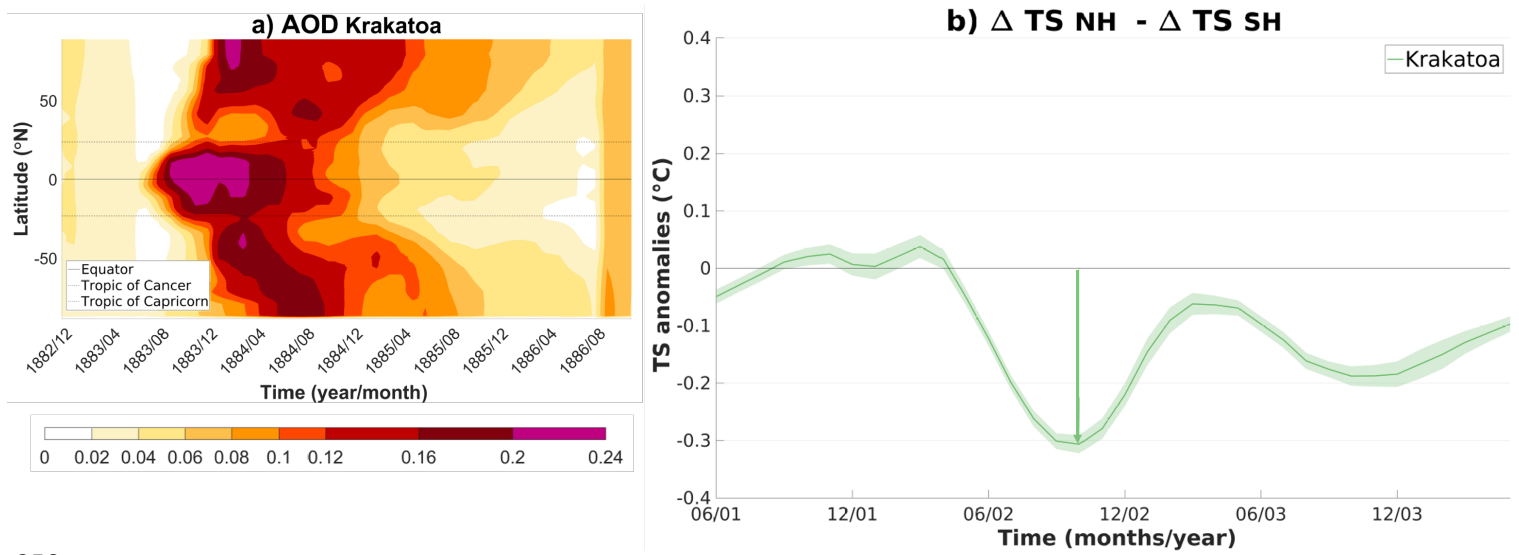
Pinatubo



335 **Figure A5.** Ensemble mean of changes in surface temperature (a,b,c,d) and precipitation (e,f,g,h) between the climatology and the volcano
 case for each seasons of the year after Pinatubo eruption. Only significant anomalies are showed with an approximate 95% confidence level
 using a Student *t*-test. Contour shows temperature and precipitations anomalies following the color bar scale (solid line for positive anomalies
 and dashed line for negative anomalies).

340

345



350

Figure A6. Evolution of the aerosol optical depth and ensemble average of the difference between the cooling of the SH ($\Delta T SH$) and the NH ($\Delta T NH$) for the Krakatau eruption. (a) The band of wavelength used is between approximately 462 nm and 625 nm. (b) 3-year climatology is subtracted to calculate the anomalies. Shading represents twice the standard error of the ensemble mean (i.e. 95% confidence interval).

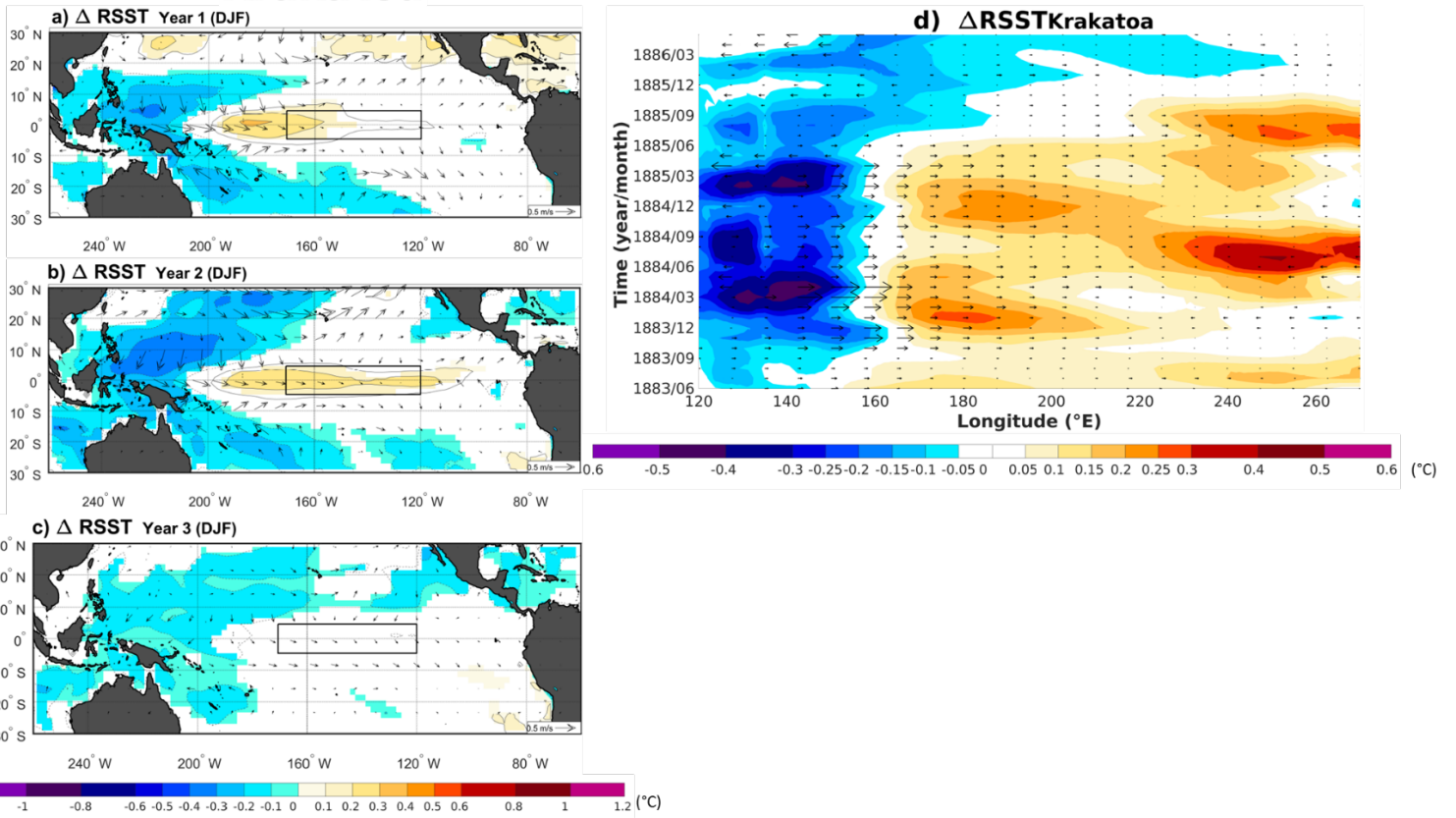
355

360

365

370

Krakatoa



375

Figure A7. Ensemble mean of changes in relative sea surface temperature anomalies and 10m winds (arrows) between the climatology and the volcano case for the three-winter season (DJF) after the Krakatau eruption. Only significant RSST changes are showed with an approximate 95 % confidence level using a Student t -test. Contours show the RSST anomalies following the color bar scale (solid lines for positive anomalies and dashed lines for negative anomalies). The boxes indicate the Niño 3.4 area.

380

385

Krakatoa

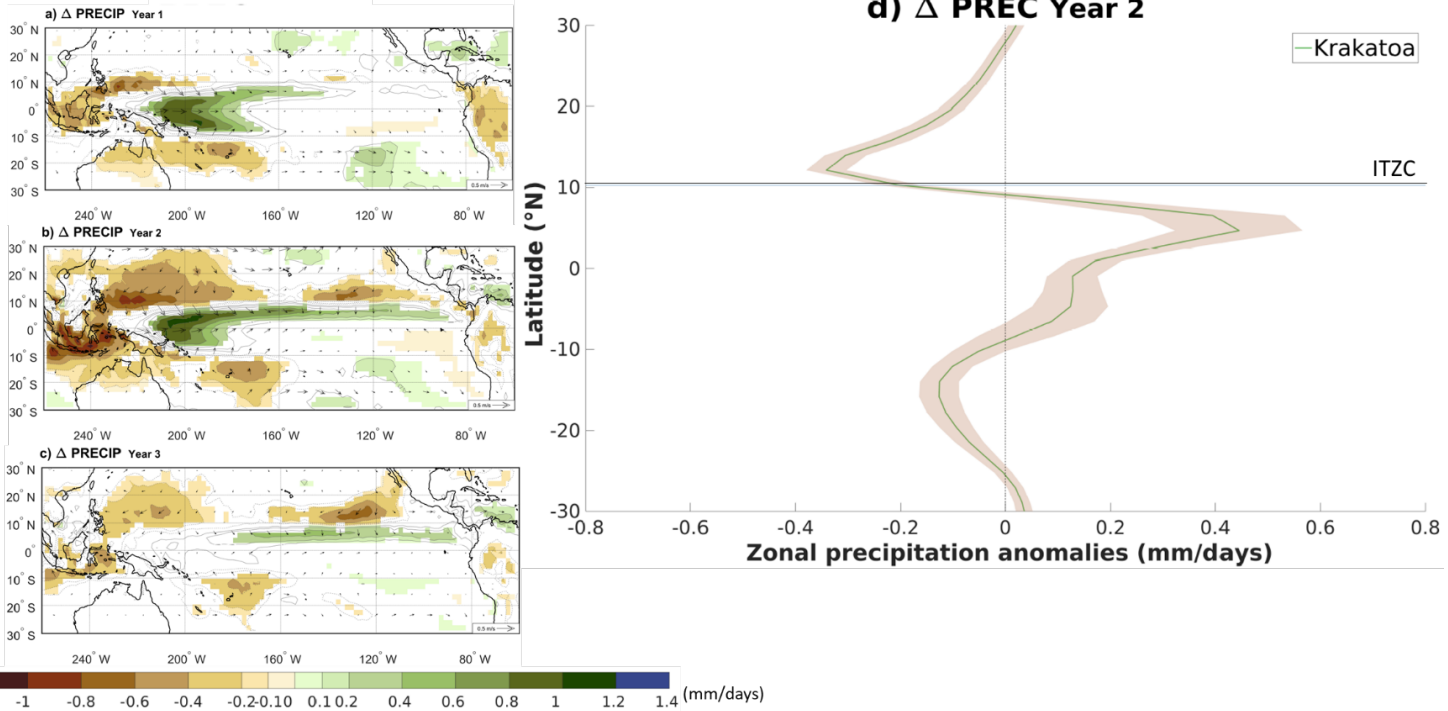
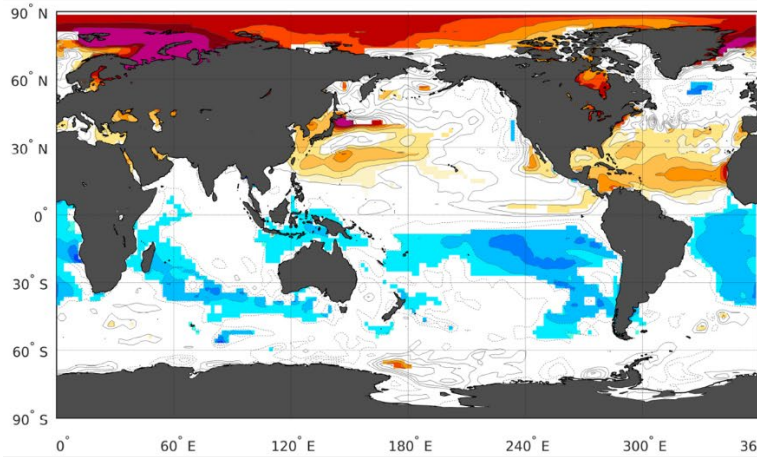


Figure A8. (a), (b), (c) Ensemble mean of changes in precipitation and 10 m wind (arrows) between the 3-year climatology and the volcano case for the three summer to winter seasons (June to February) following the Krakatau eruption. Only precipitation changes that are significant at the 95% confidence level using a Student *t*-test are shaded. Contours show the precipitation anomaly following the color bar scale (solid lines for positive anomalies and dashed lines for negative anomalies, the 0 line is omitted). (d) Ensemble average of the zonal precipitation anomaly over the Pacific Ocean (160 °E-100 °W) between the 3-year climatology and the summer to winter season (June to February) of the second year after the Krakatau eruption. Shading represents twice the standard error of the ensemble mean (i.e. 95% confidence interval). The blue line highlights the ensemble-averaged 3-year climatology position of the ITCZ (defined as the location of the zonal-average precipitation maximum).

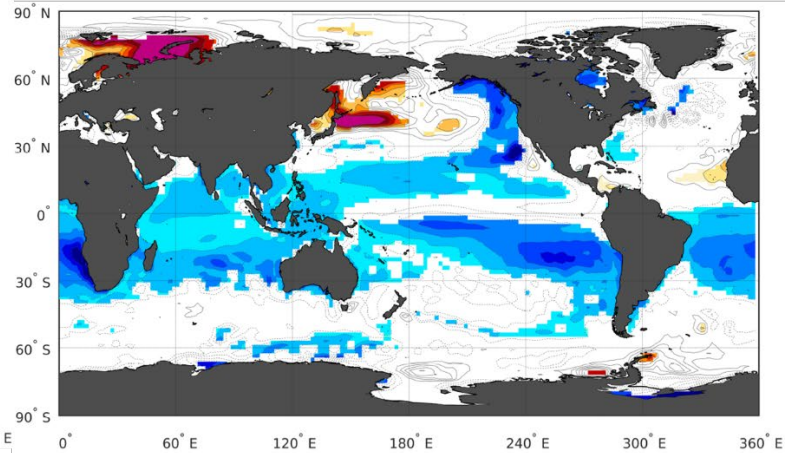
Figure A9. Difference in the ensemble mean sea surface temperature anomalies between the Pinatubo and El Chichón eruptions. ($\Delta TS_{\text{Pinatubo}} -$

$$\Delta SST_{\text{Pinatubo}} - \Delta SST_{\text{Chichon}}$$

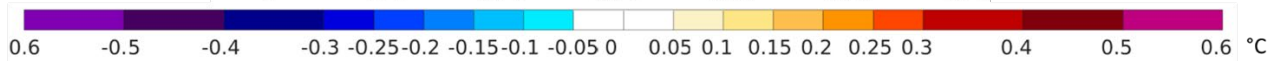
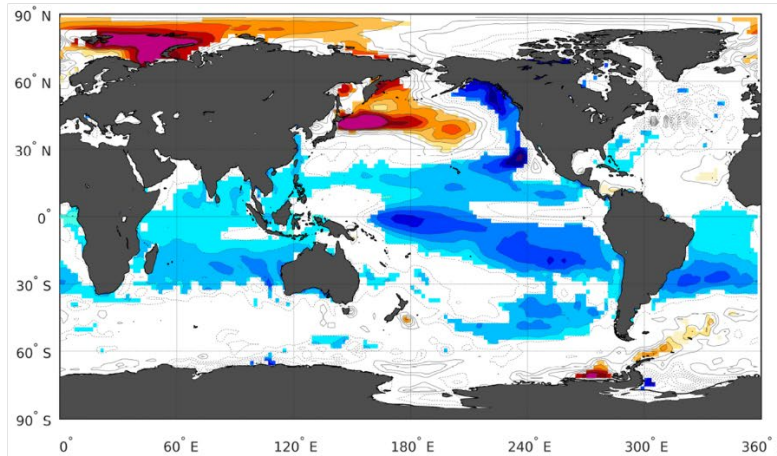
a) Year 1



b) Year 2



c) Year 3



$\Delta TS_{\text{Chichón}}$). Only significant anomalies are showed with an approximate 95% confidence level using a Student t -test. Contour shows temperature anomalies following the color bar scale (solid line for positive anomalies and dashed line for negative anomalies).

410

$\Delta\text{SLP}_{\text{Year 1 (JJA)}}$

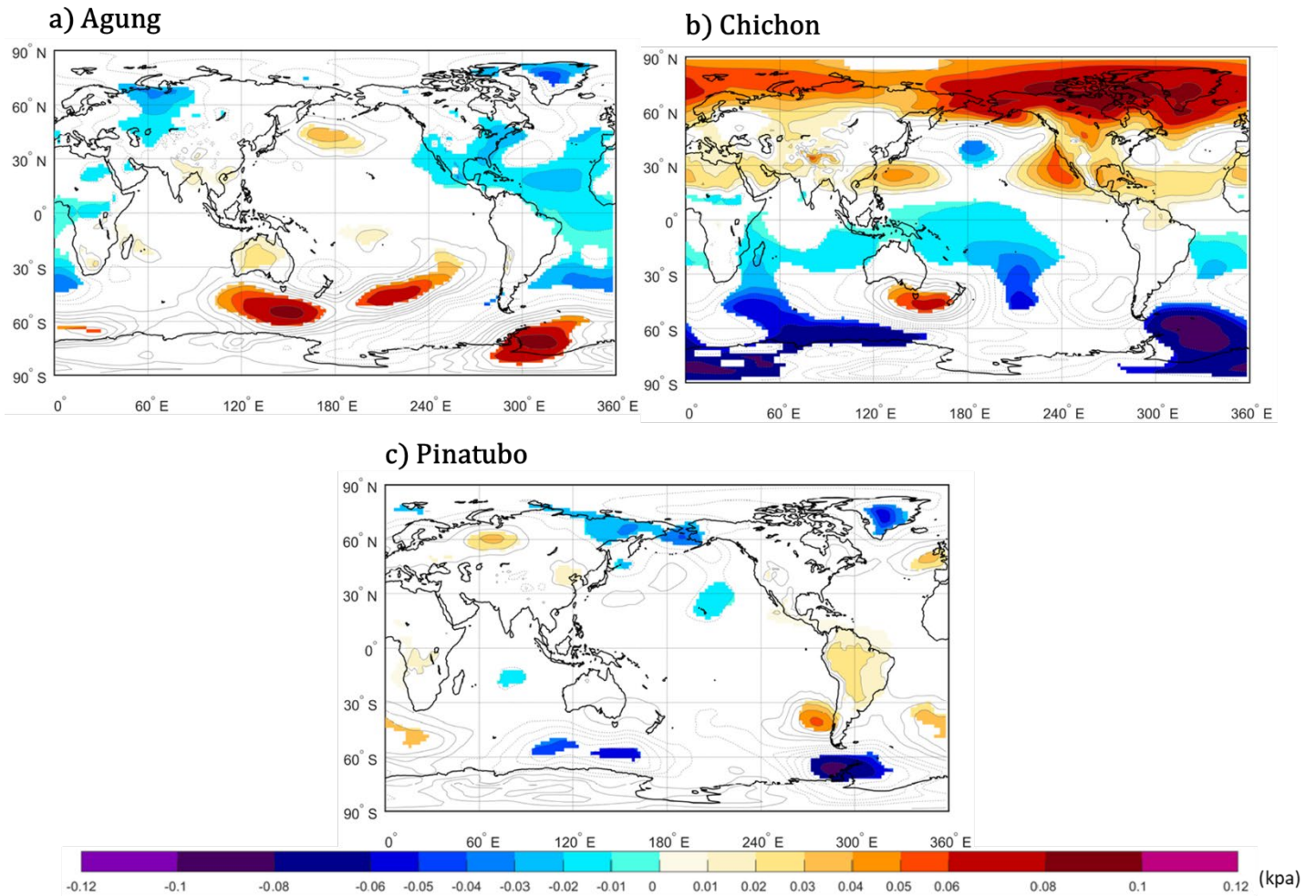
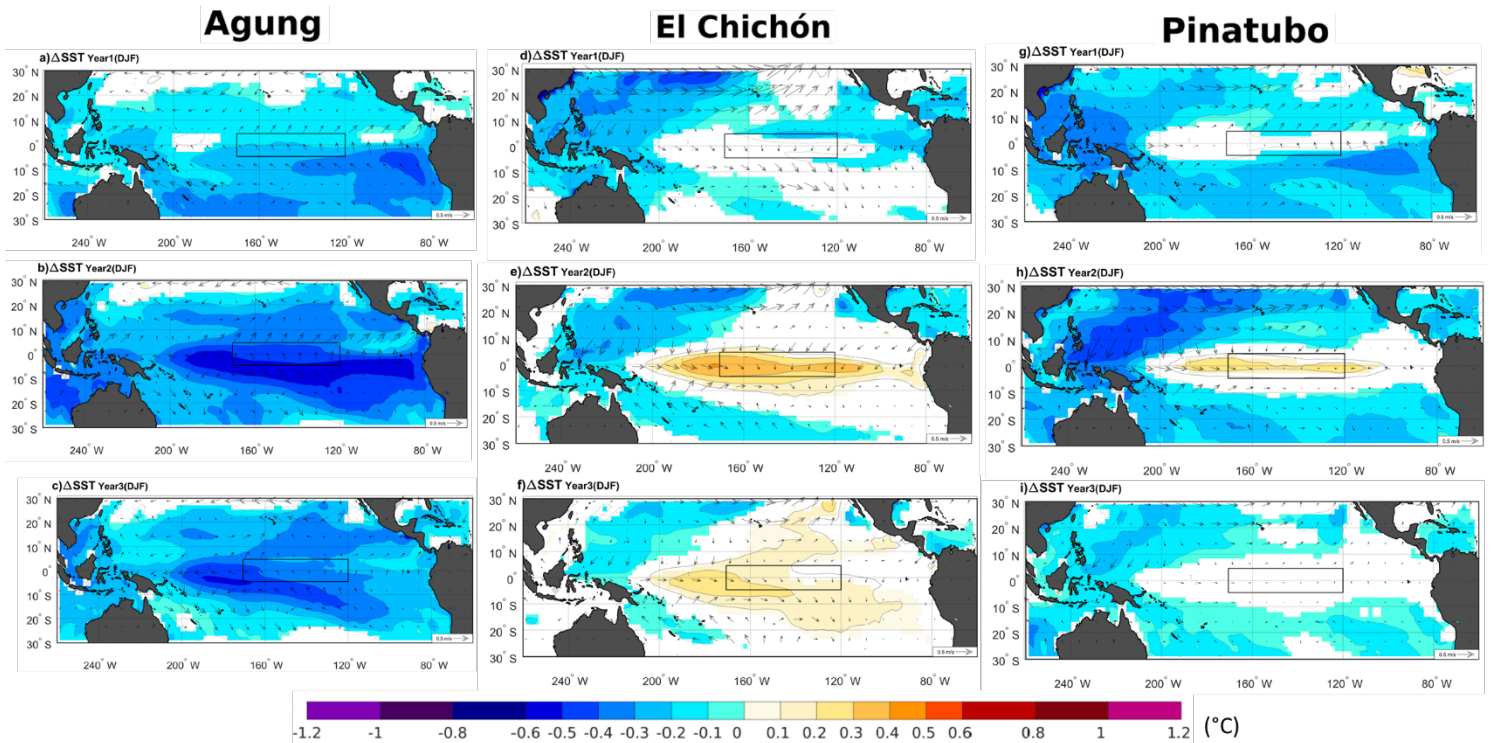


Figure A10. Ensemble average of change in the sea level pressure between the climatology and the volcano case for the first summer after Agung (a), El Chichón (b) and Pinatubo (c) eruptions. Only significant anomalies are showed with an approximate 95% confidence level using a Student *t*-test. Contour shows SLP anomalies following the color bar scale (solid line for positive anomalies and dashed line for negative anomalies).

415

420



425 **Figure A11. Ensemble mean of changes in sea surface temperature (SST) (shadings) and 10 m winds (arrows) between the volcano case and the climatology for each of the following three winter season (DJF) after the Agung (a-c), El Chichón (d-f) and the Pinatubo (g-i) eruptions. Only significant SST changes are shaded with an approximate 95 % confidence level using a Student t-test. Contours show the SST anomalies following the color bar scale (solid lines for positive anomalies and dashed lines for negative anomalies, the 0 line is omitted). The boxes indicate the Niño 3.4 area**

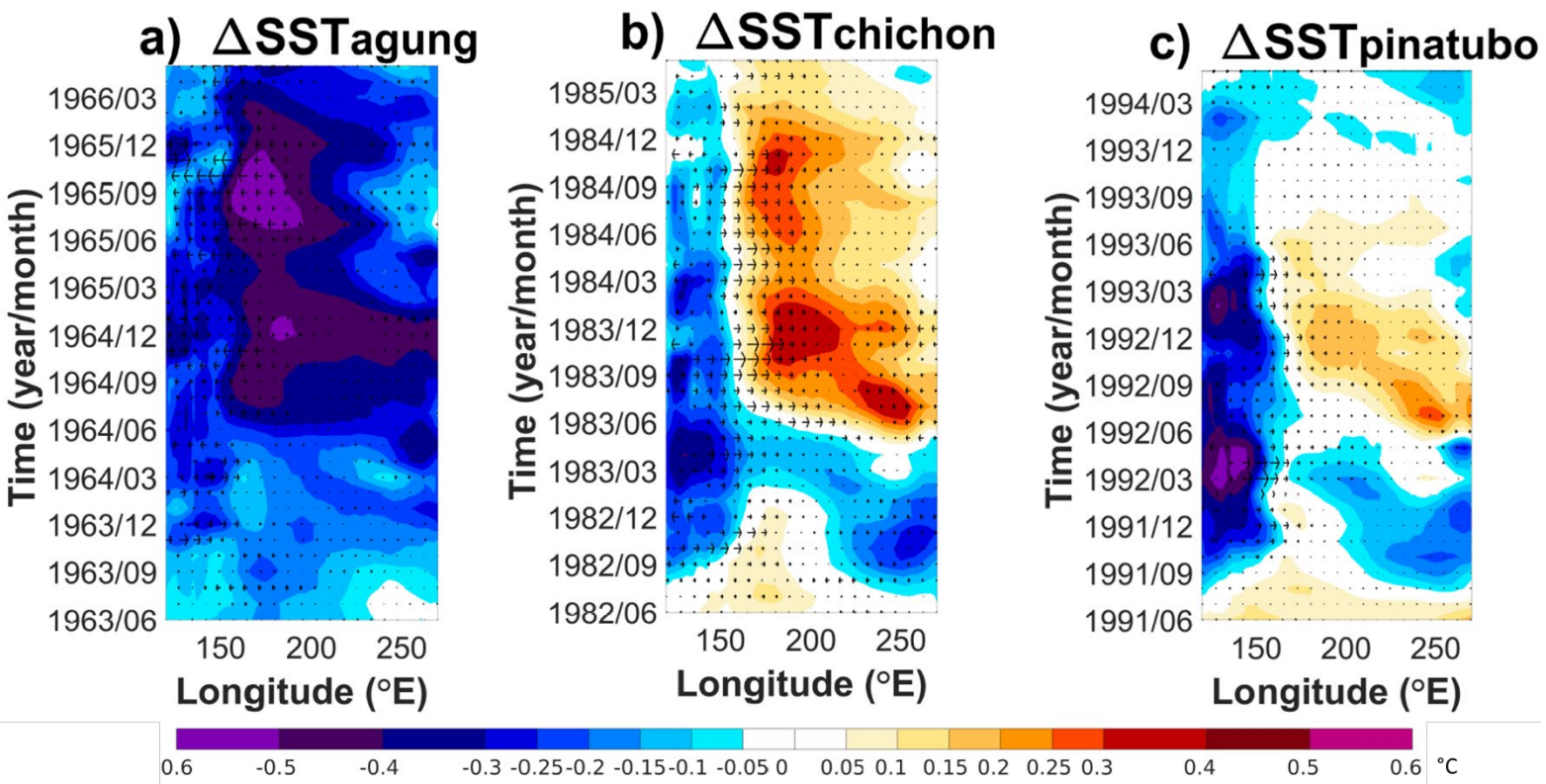
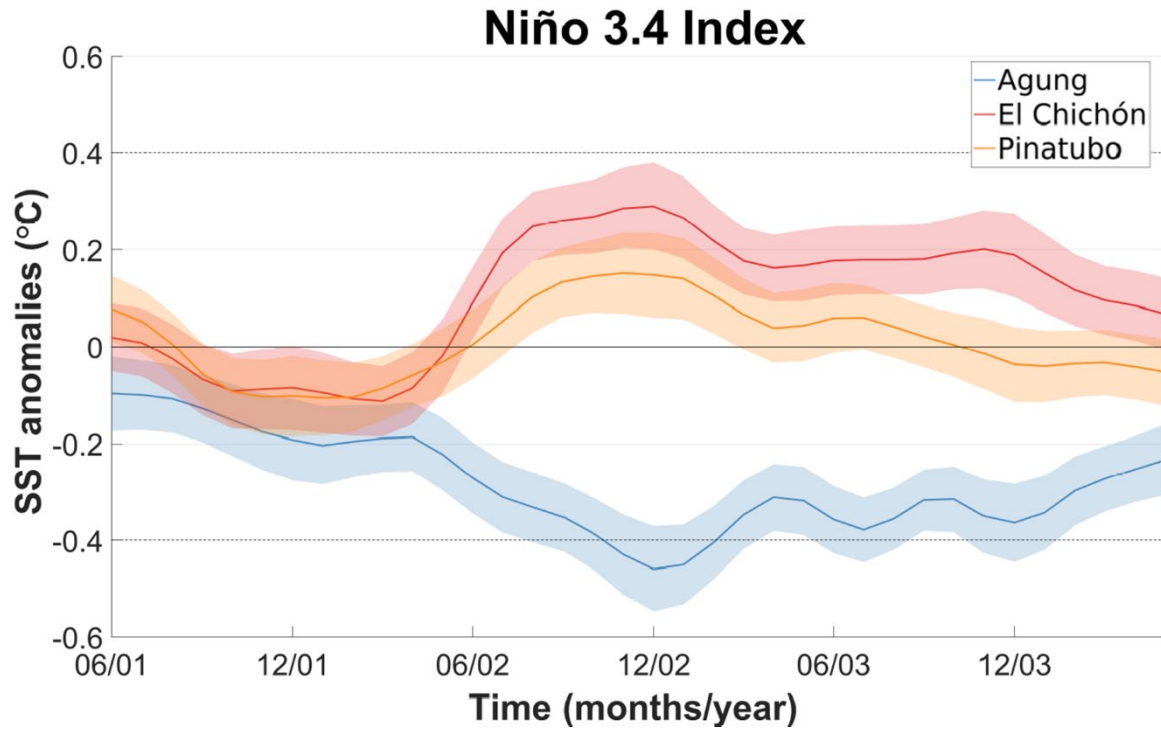


Figure A12. Hovmöller plot of the ensemble mean of the SST anomalies in the equatorial Pacific (averaged over -5°N and 5°N) and the change in the zonal component of the 10 m winds (m/s) for the three years following each eruption. The anomalies are calculated relative to the three years before each eruption.

430



435 **Figure A13: Ensemble mean changes in the Niño 3.4 index after each eruption. The 3-year climatology is subtracted to calculate the anomalies. Shading represent twice the standard error of the mean using an approximate 95% confidence interval.**

440

445

450

Agung

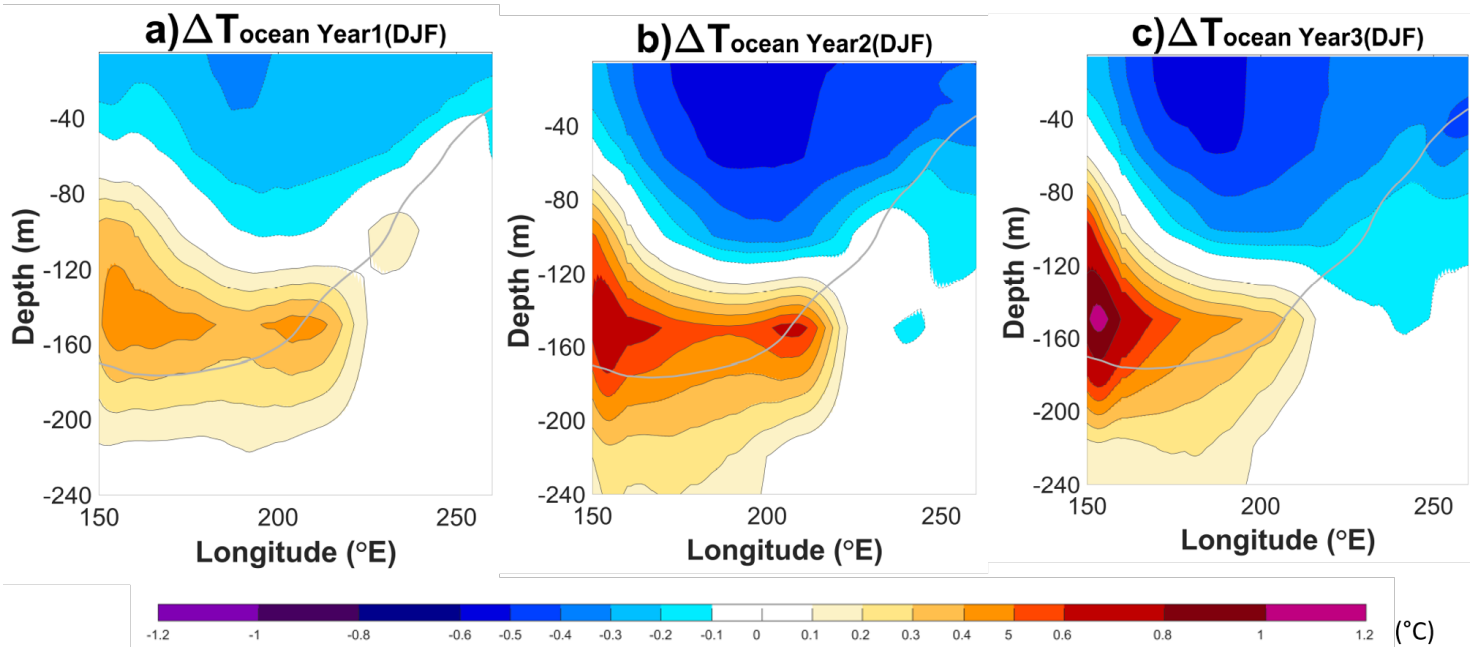
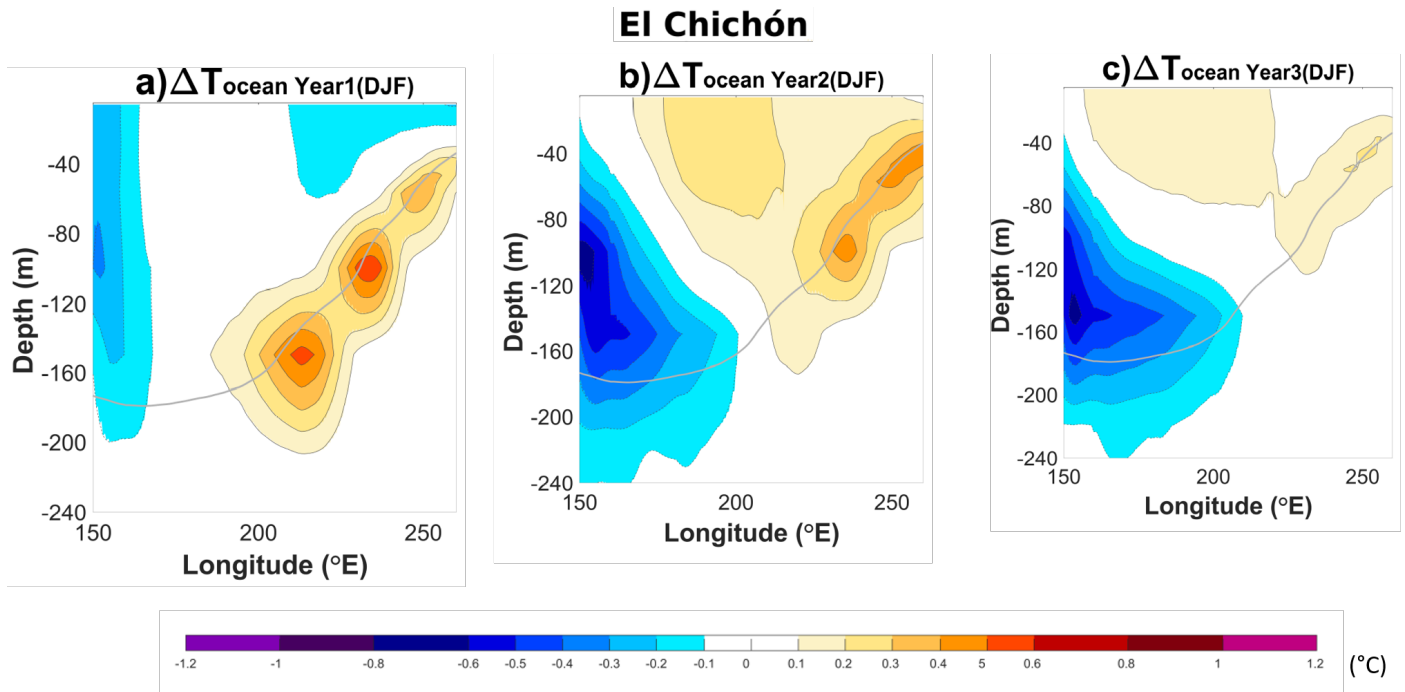


Figure A14. Ensemble mean changes shown for a transect in the equatorial Pacific (averaged $5^{\circ}\text{N} - 5^{\circ}\text{S}$) of the ocean temperature (shadings) between the volcano case and the climatology for each of the following three winter season (DJF) after the Agung eruption. Contours show the SST anomalies following the color bar scale (solid lines for positive anomalies and dashed lines for negative anomalies, the 0 line is omitted). The bold grey line shows the climatological thermocline depth (as defined using the 20°C isotherm). This is shown for 100 ensemble members.

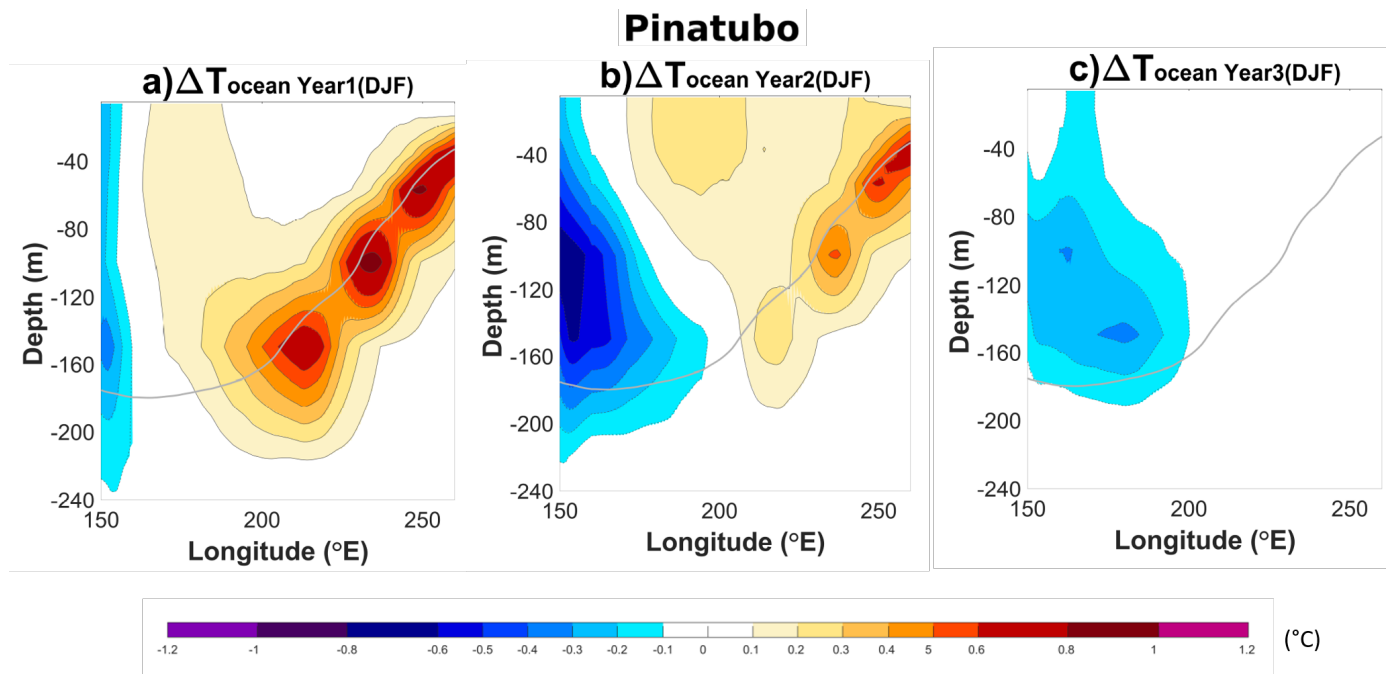
460

465

470



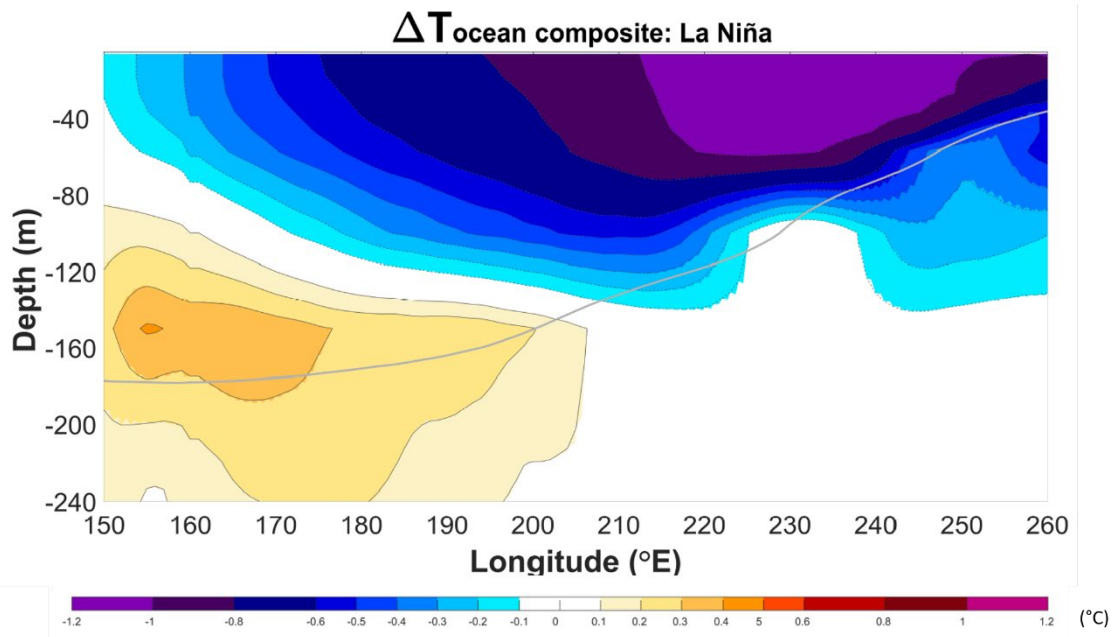
475 **Figure A15. Ensemble mean changes shown for a transect in the equatorial Pacific (averaged $5^{\circ}\text{N} - 5^{\circ}\text{S}$) of the ocean temperature (shadings) between the volcano case and the climatology for each of the following three winter season (DJF) after the Chichón eruption. Contours show the SST anomalies following the color bar scale (solid lines for positive anomalies and dashed lines for negative anomalies, the 0 line is omitted). The bold grey line shows the climatological thermocline depth (as defined using the 20°C isotherm). This is shown for 100 ensemble members.**



480 **Figure A16. Ensemble mean changes shown for a transect in the equatorial Pacific (averaged 5°N – 5°S) of the ocean temperature (shadings) between the volcano case and the climatology for each of the following three winter season (DJF) after the Pinatubo eruption. Contours show the SST anomalies following the color bar scale (solid lines for positive anomalies and dashed lines for negative anomalies, the 0 line is omitted). The bold grey line shows the climatological thermocline depth (as defined using the 20°C isotherm). This is shown for 100 ensemble members.**

485

490



495 **Figure A17. Temperature composite of La Nina events (Nino3.4 index < - 0.4°C) for a transect in the equatorial Pacific (averaged between 5°S and 5°N) in the reference period of each eruptions (4 years before each eruptions) and for the winter season (DJF). 100 ensemble members are considered, leading to a total of 1200 year as reference period and 237 La Niña events. Contours show the SST anomalies following the colorbar scale (solid lines for positive anomalies and dashed lines for negative anomalies, the 0 line is omitted). The bold grey line shows the climatological thermocline depth (as defined using the 20°C isotherm).**

500 **Author contribution**

BW analysed the model output and wrote the manuscript with support of FSRP and NM. FSRP conceived the study and supervised the findings of this work. NM provided the model output. All authors contributed to the interpretation of the results and the writing of the manuscript.

Competing interest

505 The authors declare that they have no conflict of interest.

Acknowledgements

We thank Mikhail Dobrynin and Johanna Baehr from the University of Hamburg for completing the second hundred MPI-GE ensemble simulations and providing the data from these simulations for use in this paper.

BW and FSRP acknowledge the financial support from the Natural Sciences and Engineering Research Council of Canada (grant RGPIN-2018-04981) and the Fonds de recherche du Québec–Nature et technologies (2020-NC-268559). NM was supported by the Max Planck Society for the Advancement of Science and the Alexander von Humboldt Foundation.

References

- Adams, J. B., Mann, M. E., & Ammann, C. M. (2003). Proxy evidence for an El Niño-like response to volcanic forcing. *Nature*.
<https://doi.org/10.1038/nature02101>
- 515 Barnes, J. E., & Hofmann, D. J. (1997). Lidar measurements of stratospheric aerosol over Mauna Loa Observatory. *Geophysical Research Letters*. <https://doi.org/10.1029/97GL01943>
- Bjerknes, J. (1969). Monthly Weather Review Atmospheric Teleconnections From the Equatorial Pacific. *Monthly Weather Review*.
- Christiansen, B. (2008). Volcanic eruptions, large-scale modes in the Northern Hemisphere, and the El Niño-Southern
520 Oscillation. *Journal of Climate*. <https://doi.org/10.1175/2007JCLI1657.1>
- Clement, A. C., Seager, R., Cane, M. A., & Zebiak, S. E. (1996). An ocean dynamical thermostat. *Journal of Climate*.
[https://doi.org/10.1175/1520-0442\(1996\)009<2190:AODT>2.0.CO;2](https://doi.org/10.1175/1520-0442(1996)009<2190:AODT>2.0.CO;2)
- Colose, C. M., LeGrande, A. N., & Vuille, M. (2016a). Hemispherically asymmetric volcanic forcing of tropical hydroclimate
during the last millennium. *Earth System Dynamics*. <https://doi.org/10.5194/esd-7-681-2016>
- 525 Colose, C. M., LeGrande, A. N., & Vuille, M. (2016b). The influence of volcanic eruptions on the climate of tropical South
America during the last millennium in an isotope-enabled general circulation model. *Climate of the Past*.
<https://doi.org/10.5194/cp-12-961-2016>
- D'Arrigo, R., Cook, E. R., Wilson, R. J., Allan, R., & Mann, M. E. (2005). On the variability of ENSO over the past six centuries.
Geophysical Research Letters. <https://doi.org/10.1029/2004GL022055>
- 530 Dee, S. G., Cobb, K. M., Emile-Geay, J., Ault, T. R., Lawrence Edwards, R., Cheng, H., & Charles, C. D. (2020). No consistent
ENSO response to volcanic forcing over the last millennium. *Science*. <https://doi.org/10.1126/science.aax2000>
- Ding, Y., Carton, J. A., Chepurin, G. A., Stenchikov, G., Robock, A., Sentman, L. T., & Krasting, J. P. (2014). Ocean response to
volcanic eruptions in Coupled Model Intercomparison Project 5 simulations. *Journal of Geophysical Research C:
Oceans*. <https://doi.org/10.1002/2013JC009780>
- 535 Driscoll, S., Bozzo, A., Gray, L. J., Robock, A., & Stenchikov, G. (2012). Coupled Model Intercomparison Project 5 (CMIP5)
simulations of climate following volcanic eruptions. *Journal of Geophysical Research Atmospheres*.
<https://doi.org/10.1029/2012JD017607>
- Eddebbar, Y. A., Rodgers, K. B., Long, M. C., Subramanian, A. C., Xie, S. P., & Keeling, R. F. (2019). El Niño-like physical and

- biogeochemical ocean response to tropical eruptions. *Journal of Climate*. <https://doi.org/10.1175/JCLI-D-18-0458.1>
- 540 Emile-Geay, J., Seager, R., Cane, M. A., Cook, E. R., & Haug, G. H. (2008). Volcanoes and ENSO over the past millennium. *Journal of Climate*. <https://doi.org/10.1175/2007JCLI1884.1>
- Giorgetta, M. A., Jungclaus, J., Reick, C. H., Legutke, S., Bader, J., Böttinger, M., et al. (2013). Climate and carbon cycle changes from 1850 to 2100 in MPI-ESM simulations for the Coupled Model Intercomparison Project phase 5. *Journal of Advances in Modeling Earth Systems*. <https://doi.org/10.1002/jame.20038>
- 545 Harshvardhan. (1979). Harshvardhan_1979_Perturbation of the Zonal Radiation Balance by a stratospheric aerosol layer. *Journal of Atmospheric Science*.pdf. *Journal of Atmospheric Sciences*. [https://doi.org/10.1175/1520-0469\(1979\)036<1274:POTZRB>2.0.CO;2](https://doi.org/10.1175/1520-0469(1979)036<1274:POTZRB>2.0.CO;2)
- Iles, C. E., Hegerl, G. C., Schurer, A. P., & Zhang, X. (2013). The effect of volcanic eruptions on global precipitation. *Journal of Geophysical Research Atmospheres*. <https://doi.org/10.1002/jgrd.50678>
- 550 Kang, S. M., Held, I. M., Frierson, D. M. W., & Zhao, M. (2008). The response of the ITCZ to extratropical thermal forcing: Idealized slab-ocean experiments with a GCM. *Journal of Climate*. <https://doi.org/10.1175/2007JCLI2146.1>
- Khodri, M., Izumo, T., Vialard, J., Janicot, S., Cassou, C., Lengaigne, M., et al. (2017). Tropical explosive volcanic eruptions can trigger El Niño by cooling tropical Africa. *Nature Communications*. <https://doi.org/10.1038/s41467-017-00755-6>
- Kodera, K. (1994). Influence of volcanic eruptions on the troposphere through stratospheric dynamical processes in the Northern Hemisphere winter. *Journal of Geophysical Research*. <https://doi.org/10.1029/93JD02731>
- 555 Li, J., Xie, S. P., Cook, E. R., Morales, M. S., Christie, D. A., Johnson, N. C., et al. (2013). El Niño modulations over the past seven centuries. *Nature Climate Change*. <https://doi.org/10.1038/nclimate1936>
- Liu, F., Li, J., Wang, B., Liu, J., Li, T., Huang, G., & Wang, Z. (2018). Divergent El Niño responses to volcanic eruptions at different latitudes over the past millennium. *Climate Dynamics*. <https://doi.org/10.1007/s00382-017-3846-z>
- 560 Liu, F., Xing, C., Sun, L., Wang, B., Chen, D., & Liu, J. (2018). How Do Tropical, Northern Hemispheric, and Southern Hemispheric Volcanic Eruptions Affect ENSO Under Different Initial Ocean Conditions? *Geophysical Research Letters*. <https://doi.org/10.1029/2018GL080315>
- Maher, N., McGregor, S., England, M. H., & Gupta, A. Sen. (2015). Effects of volcanism on tropical variability. *Geophysical Research Letters*. <https://doi.org/10.1002/2015GL064751>
- 565 Maher, N., Milinski, S., Suarez-Gutierrez, L., Botzet, M., Dobrynin, M., Kornblueh, L., et al. (2019). The Max Planck Institute Grand Ensemble - Enabling the Exploration of Climate System Variability. *Journal of Advances in Modeling Earth Systems*. <https://doi.org/10.1029/2019MS001639>
- Man, W., Zhou, T., & Jungclaus, J. H. (2014). Effects of large volcanic eruptions on global summer climate and east asian monsoon changes during the last millennium: Analysis of MPI-ESM simulations. *Journal of Climate*. <https://doi.org/10.1175/JCLI-D-13-00739.1>
- 570

- McGregor, S., Timmermann, A., & Timm, O. (2010). A unified proxy for ENSO and PDO variability since 1650. *Climate of the Past*. <https://doi.org/10.5194/cp-6-1-2010>
- McGregor, Shayne, & Timmermann, A. (2011). The effect of explosive tropical volcanism on ENSO. *Journal of Climate*. <https://doi.org/10.1175/2010JCLI3990.1>
- 575 McGregor, Shayne, Khodri, M., Maher, N., Ohba, M., Pausata, F. S. R., & Stevenson, S. (2020). The Effect of Strong Volcanic Eruptions on ENSO. <https://doi.org/10.1002/9781119548164.ch12>
- Milinski, S., Maher, N., & Olonscheck, D. (2019). How large does a large ensemble need to be? *Earth System Dynamics Discussions*. <https://doi.org/10.5194/esd-2019-70>
- Ohba, M., Shiogama, H., Yokohata, T., & Watanabe, M. (2013). Impact of strong tropical volcanic eruptions on ENSO simulated in a coupled GCM. *Journal of Climate*. <https://doi.org/10.1175/JCLI-D-12-00471.1>
- 580 Paik, S., Min, S. K., Iles, C. E., Fischer, E. M., & Schurer, A. P. (2020). Volcanic-induced global monsoon drying modulated by diverse El Niño responses. *Science Advances*. <https://doi.org/10.1126/sciadv.aba1212>
- Pausata, F. S. R., Grini, A., Caballero, R., Hannachi, A., & Seland, Ø. (2015). High-latitude volcanic eruptions in the Norwegian Earth System Model: The effect of different initial conditions and of the ensemble size. *Tellus, Series B: Chemical and Physical Meteorology*. <https://doi.org/10.3402/tellusb.v67.26728>
- 585 Pausata, F. S. R., Chafik, L., Caballero, R., & Battisti, D. S. (2015). Impacts of high-latitude volcanic eruptions on ENSO and AMOC. *Proceedings of the National Academy of Sciences*. <https://doi.org/10.1073/pnas.1509153112>
- Pausata, F. S. R., Karamperidou, C., Caballero, R., & Battisti, D. S. (2016). ENSO response to high-latitude volcanic eruptions in the Northern Hemisphere: The role of the initial conditions. *Geophysical Research Letters*. <https://doi.org/10.1002/2016GL069575>
- 590 Pinto, J. P., Turco, R. P., & Toon, O. B. (1989). Self-limiting physical and chemical effects in volcanic eruption clouds. *Journal of Geophysical Research*. <https://doi.org/10.1029/jd094id08p11165>
- Pollack, J. B., Toon, O. B., Sagan, C., Summers, A., Baldwin, B., & Van Camp, W. (1976). Volcanic explosions and climatic change: A theoretical assessment. *Journal of Geophysical Research*. <https://doi.org/10.1029/jc081i006p01071>
- 595 Predybaylo, E., Stenchikov, G. L., Wittenberg, A. T., & Zeng, F. (2017). Impacts of a pinatubo-size volcanic eruption on ENSO. *Journal of Geophysical Research*. <https://doi.org/10.1002/2016JD025796>
- Rampino, M. R., & Self, S. (1984). Sulphur-rich volcanic eruptions and stratospheric aerosols. *Nature*. <https://doi.org/10.1038/310677a0>
- 600 Robock, A. (2000). Volcanic eruptions and climate. *Reviews of Geophysics*. <https://doi.org/10.1029/1998RG000054>
- Robock, A., & Yuhua Liu. (1994). The volcanic signal in Goddard Institute for Space Studies three-dimensional model

- simulations. *Journal of Climate*. [https://doi.org/10.1175/1520-0442\(1994\)007<0044:TVSIGI>2.0.CO;2](https://doi.org/10.1175/1520-0442(1994)007<0044:TVSIGI>2.0.CO;2)
- 605 Schneider, T., Bischoff, T., & Haug, G. H. (2014). Migrations and dynamics of the intertropical convergence zone. *Nature*.
<https://doi.org/10.1038/nature13636>
- Self, S., Rampino, M. R., Zhao, J., & Katz, M. G. (1997). Volcanic aerosol perturbations and strong El Niño events: No general correlation. *Geophysical Research Letters*. <https://doi.org/10.1029/97GL01127>
- Stechmann, S. N., & Ogrosky, H. R. (2014). The Walker circulation, diabatic heating, and outgoing longwave radiation. *Geophysical Research Letters*. <https://doi.org/10.1002/2014GL062257>
- 610 Stenchikov, G., Hamilton, K., Stouffer, R. J., Robock, A., Ramaswamy, V., Santer, B., & Graf, H. F. (2006). Arctic Oscillation response to volcanic eruptions in the IPCC AR4 climate models. *Journal of Geophysical Research Atmospheres*.
<https://doi.org/10.1029/2005JD006286>
- Stenchikov, G. L., Kirchner, I., Robock, A., Graf, H. F., Antuña, J. C., Grainger, R. G., et al. (1998). Radiative forcing from the 1991 Mount Pinatubo volcanic eruption. *Journal of Geophysical Research Atmospheres*.
- 615 <https://doi.org/10.1029/98JD00693>
- Stevenson, S., Otto-Bliesner, B., Fasullo, J., & Brady, E. (2016). “El Niño Like” hydroclimate responses to last millennium volcanic eruptions. *Journal of Climate*. <https://doi.org/10.1175/JCLI-D-15-0239.1>
- Stevenson, S., Fasullo, J. T., Otto-Bliesner, B. L., Tomas, R. A., & Gao, C. (2017). Role of eruption season in reconciling model and proxy responses to tropical volcanism. *Proceedings of the National Academy of Sciences*.
- 620 <https://doi.org/10.1073/pnas.1612505114>
- Sun, W., Liu, J., Wang, B., Chen, D., Liu, F., Wang, Z., et al. (2019). A “La Niña-like” state occurring in the second year after large tropical volcanic eruptions during the past 1500 years. *Climate Dynamics*. <https://doi.org/10.1007/s00382-018-4163-x>
- Thompson, D. W. J., Wallace, J. M., Jones, P. D., & Kennedy, J. J. (2009). Identifying signatures of natural climate variability in time series of global-mean surface temperature: Methodology and insights. *Journal of Climate*.
- 625 <https://doi.org/10.1175/2009JCLI3089.1>
- Timmreck, C. (2012). Modeling the climatic effects of large explosive volcanic eruptions. *Wiley Interdisciplinary Reviews: Climate Change*. <https://doi.org/10.1002/wcc.192>
- Trenberth, K. E., & Dai, A. (2007). Effects of Mount Pinatubo volcanic eruption on the hydrological cycle as an analog of
- 630 geoengineering. *Geophysical Research Letters*. <https://doi.org/10.1029/2007GL030524>
- Wilson, R., Cook, E., D’arrigo, R., Riedwyl, N., Evans, M. N., Tudhope, A., & Rob, A. (2010). Reconstructing ENSO: The influence of method, proxy data, climate forcing and teleconnections. *Journal of Quaternary Science*.
<https://doi.org/10.1002/jqs.1297>
- Wittenberg, A. T. (2009). Are historical records sufficient to constrain ENSO simulations? *Geophysical Research Letters*.

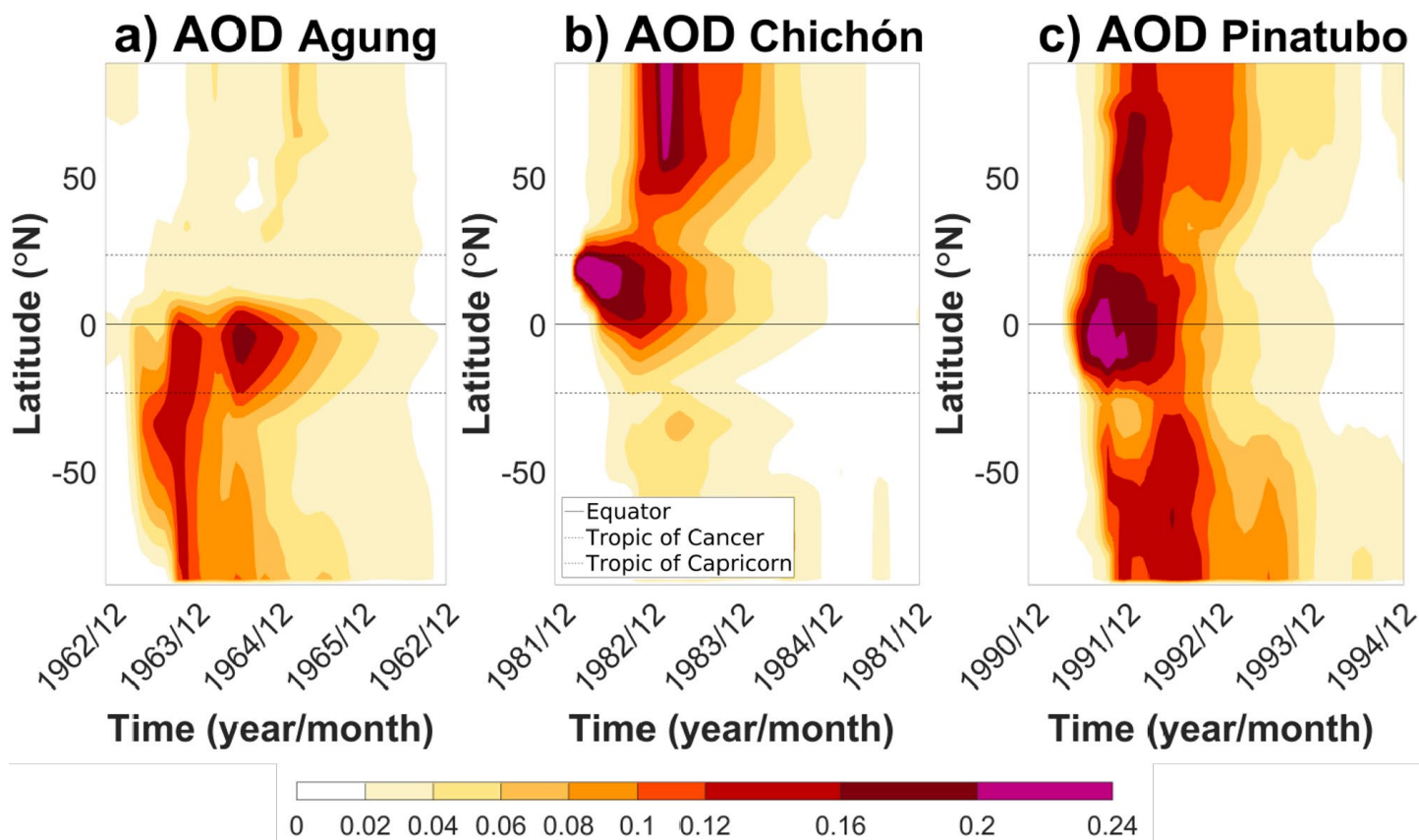
Zambri, B., & Robock, A. (2016). Winter warming and summer monsoon reduction after volcanic eruptions in Coupled Model Intercomparison Project 5 (CMIP5) simulations. *Geophysical Research Letters*.

<https://doi.org/10.1002/2016GL070460>

640 Zanchettin, D., Timmreck, C., Graf, H. F., Rubino, A., Lorenz, S., Lohmann, K., et al. (2012). Bi-decadal variability excited in the coupled ocean-atmosphere system by strong tropical volcanic eruptions. *Climate Dynamics*.

<https://doi.org/10.1007/s00382-011-1167-1>

Zuo, M., Man, W., Zhou, T., & Guo, Z. (2018). Different impacts of Northern, tropical, and Southern volcanic eruptions on the tropical pacific SST in the Last Millennium. *Journal of Climate*. <https://doi.org/10.1175/JCLI-D-17-0571.1>



645 **Figure 1.** Evolution of the aerosol optical depth during four years for the three eruptions. The band of wavelength used is between approximately 462 nm and 625 nm.

Agung

El Chichón

Pinatubo

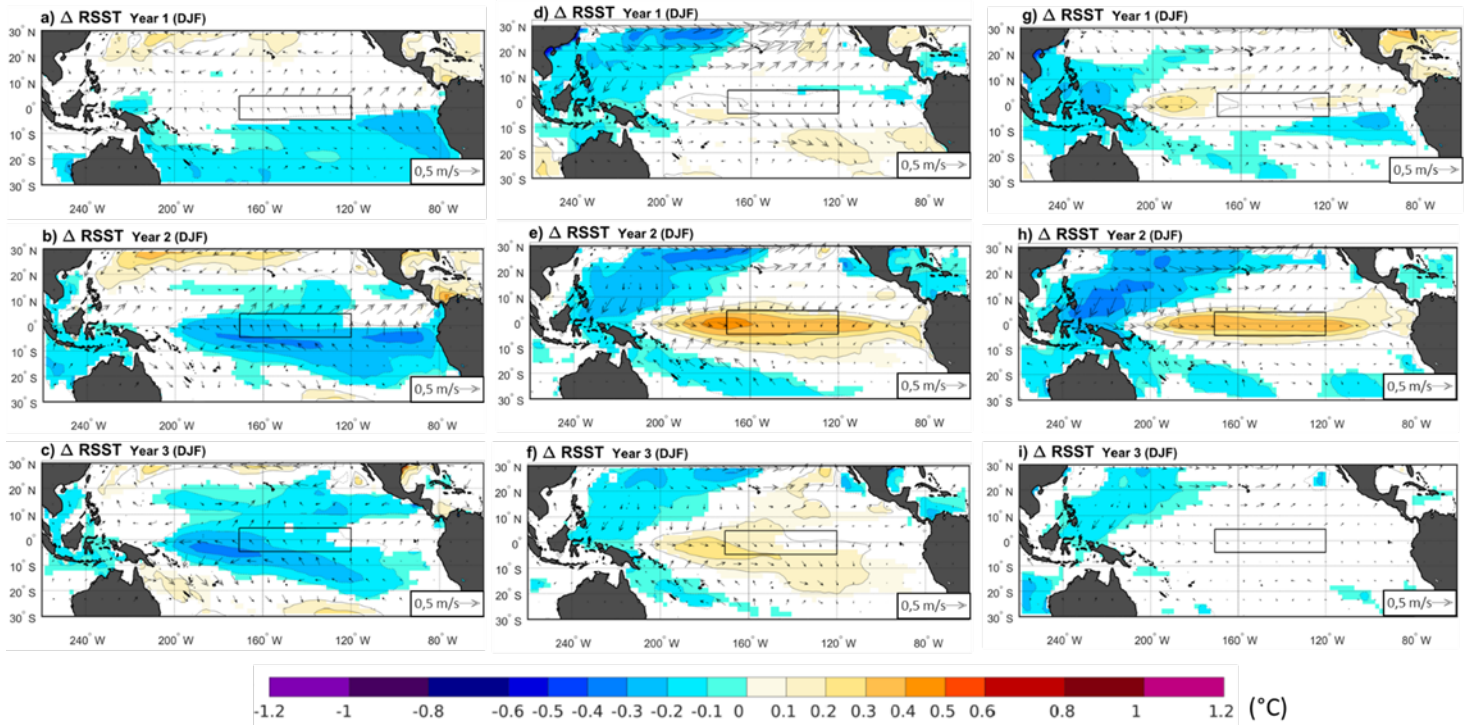


Figure 2. Ensemble mean of changes in relative sea surface temperature (RSST) (shadings) and 10 m winds (arrows) between the volcano case and the climatology for each of the following three winter season (DJF) after the Agung (a-c), El Chichón (d-f) and the Pinatubo (g-i) eruptions. Only significant RSST changes are shaded with an approximate 95 % confidence level using a Student t-test. Contours show the RSST anomalies following the color bar scale (solid lines for positive anomalies and dashed lines for negative anomalies, the 0 line is omitted). The boxes indicate the Niño 3.4 area.

650

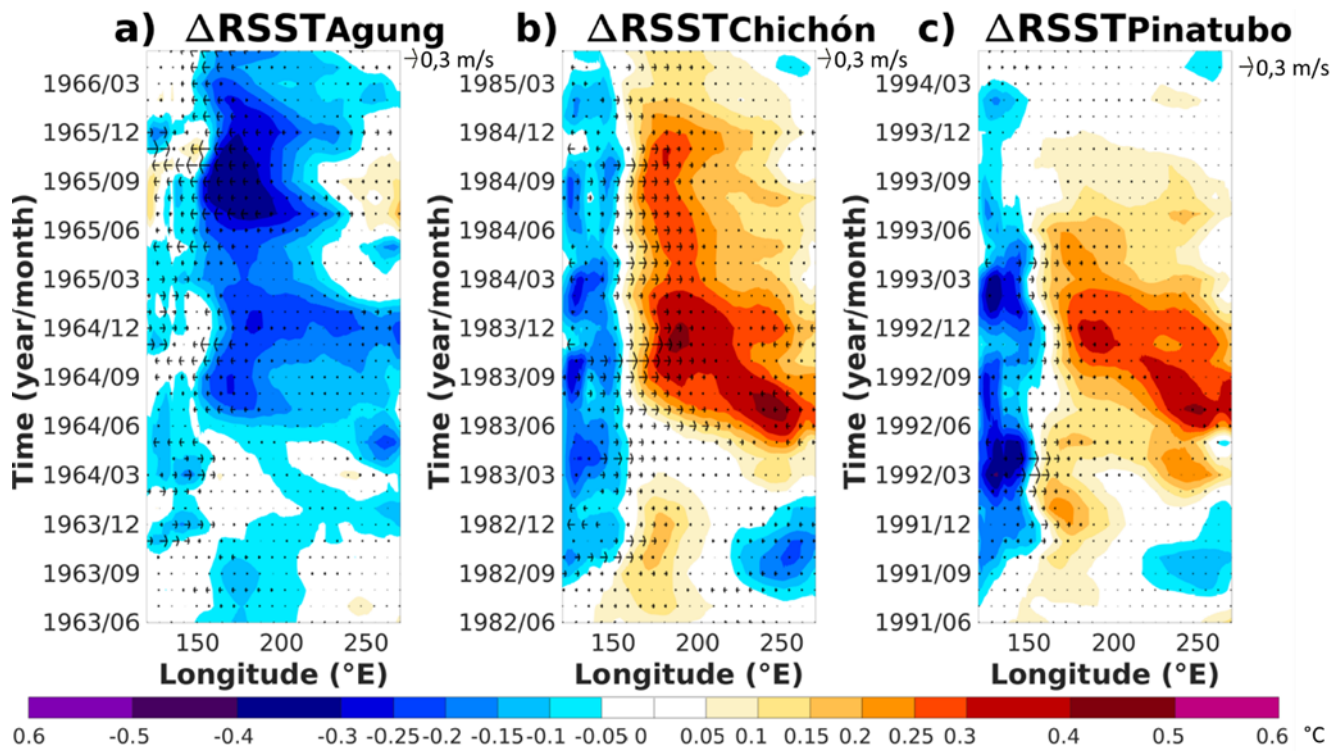


Figure 3. Hovmöller plot of the ensemble mean of the relative SST anomalies in the equatorial Pacific (averaged over -5°N and 5°N) and the change in the zonal component of the 10 m winds (m/s) for the three years following each eruption. The anomalies are calculated relative to the three years before each eruption.

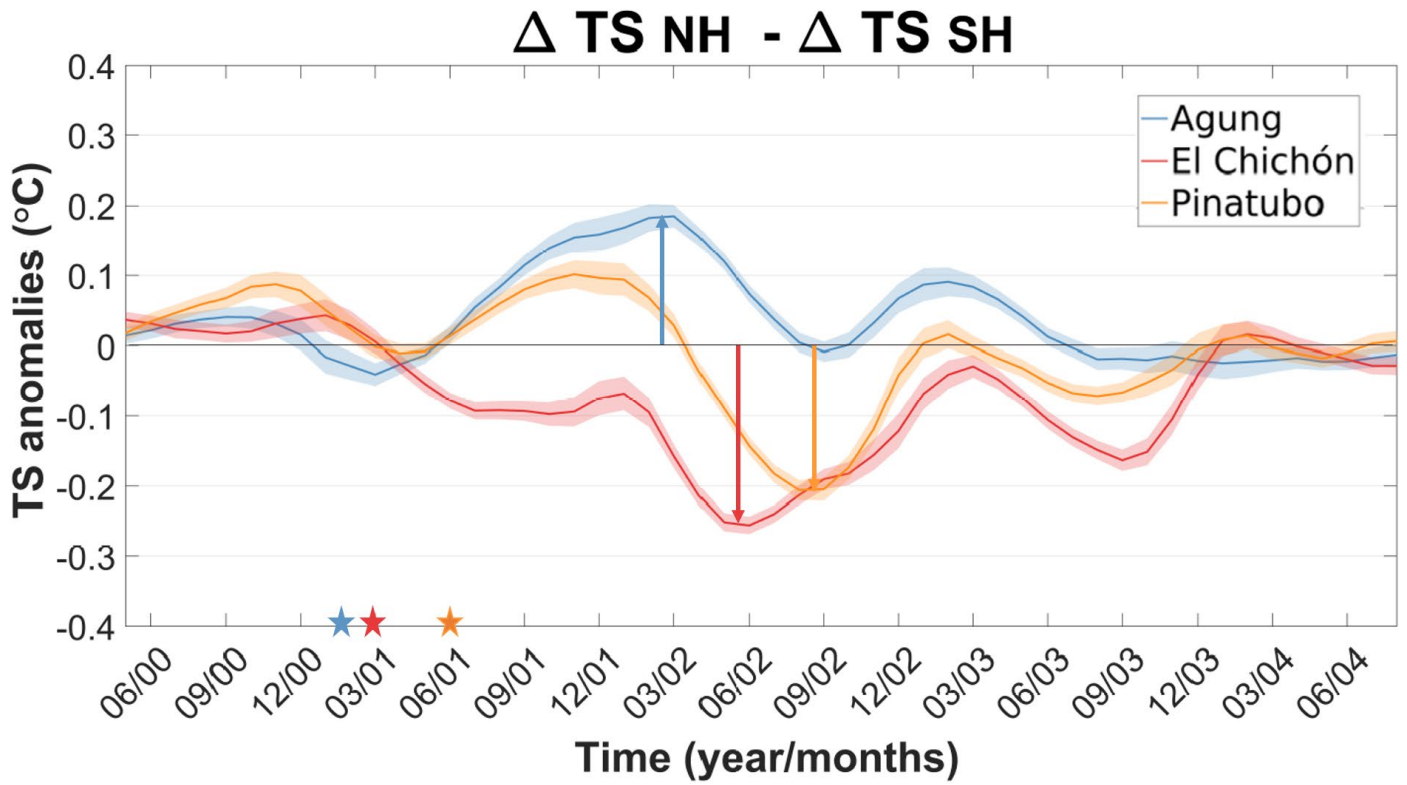


Figure 4. Evolution of the difference in the ensemble mean between the volcanically induced cooling of the SH and the NH after each eruption ($\Delta T_{NH} - \Delta T_{SH}$). Shading represents twice the standard error of the ensemble mean (i.e. $\pm 95\%$ confidence interval).

Agung

El Chichón

Pinatubo

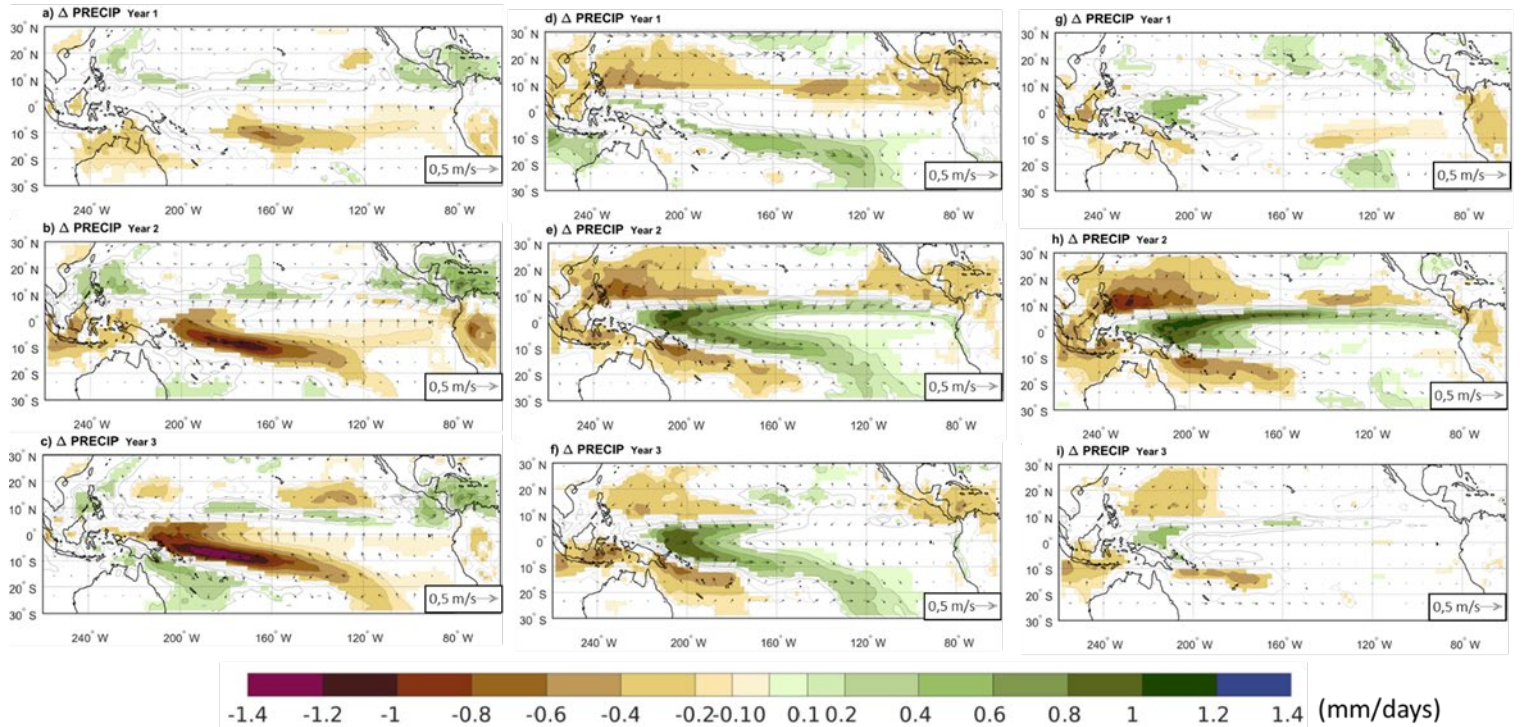


Figure 5. Change in ensemble mean precipitation and 10 m winds (arrows) between the references years and the volcano case for the three summer to winter seasons (June to February) following the Agung (a-c), El Chichón (d-f) and the Pinatubo (g-i) eruptions. Contours show the precipitation anomaly following the color bar scale (solid lines for positive anomalies and dashed lines for negative anomalies, the 0 line is omitted). Only precipitation changes that are significant at the 95% confidence level using a Student t-test are shaded.

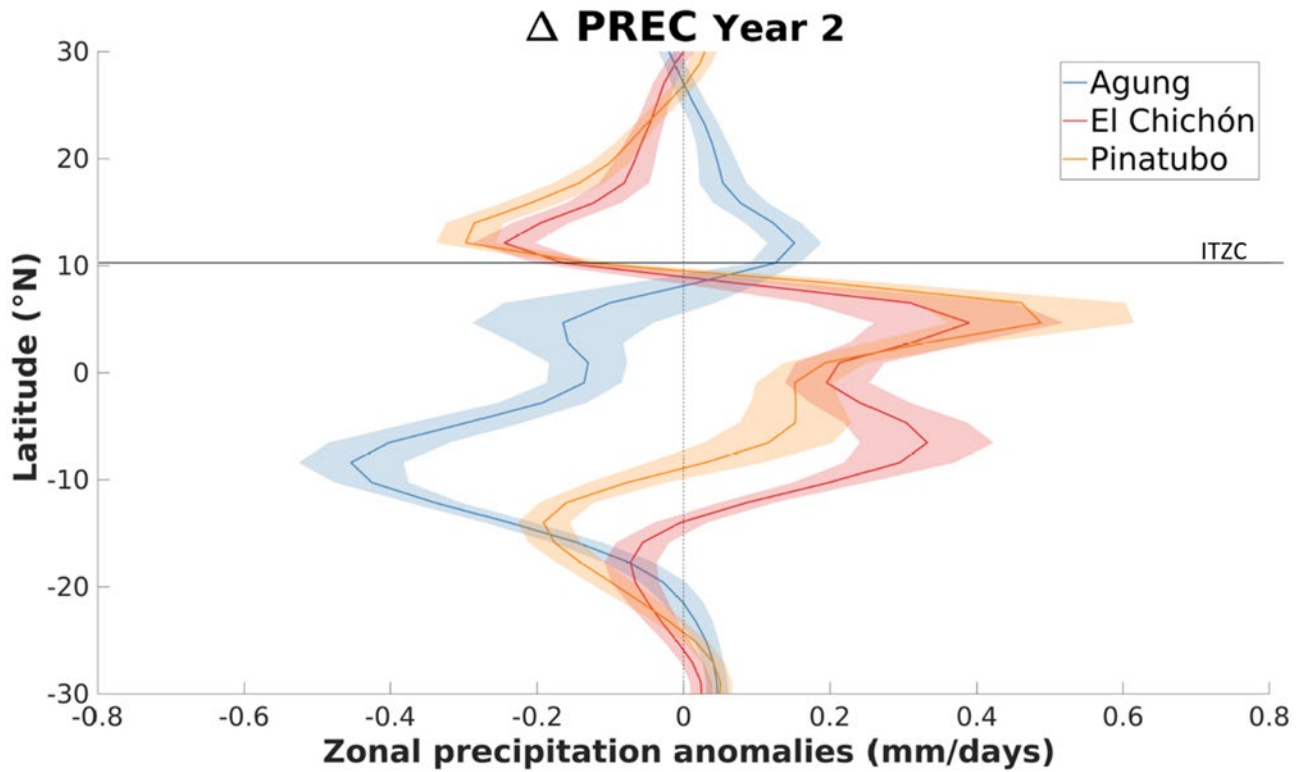


Figure 6. Ensemble mean of the zonal precipitation anomaly over the Pacific Ocean (160 °E-100 °W) between the summer to winter seasons (June to February) of the second year after each eruption and the 3-year climatology. Shading represents twice the standard error of the ensemble mean (i.e. 95% confidence interval). The horizontal line highlights the ensemble-mean 3-year climatology position of the ITCZ (defined as the location of the zonal-average precipitation maximum).

670

PAi V - PAi NV

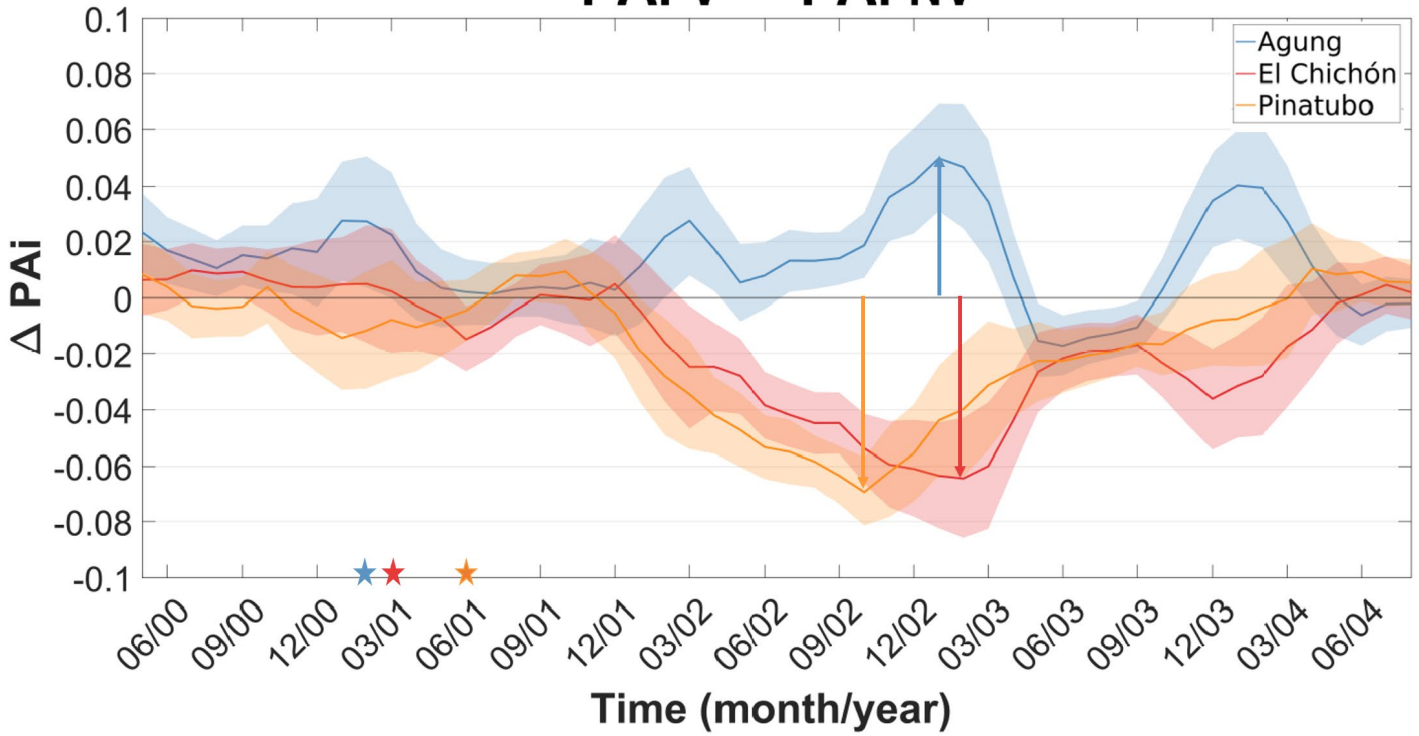


Figure 7. Evolution of the difference in the ensemble mean between the precipitation asymmetry index (PAi) after each eruption (PAi_V), and the climatology (PAi_{NV}). Shading represents twice the standard error of the ensemble mean (i.e. 95% confidence interval). The three stars represent the moment of each eruption.